

# An Engineered Biosynthetic-Synthetic Platform for Production of Halogenated Indolmycin Antibiotics

Elesha R. Hoffarth,<sup>1</sup> Sunnie Kong,<sup>1</sup> Hai-Yan He,<sup>1,2</sup> Katherine S. Ryan\*

<sup>1</sup>Department of Chemistry, The University of British Columbia, Vancouver, Canada

<sup>2</sup>Current address: Institute of Medicinal Biotechnology, Chinese Academy of Medical Sciences & Peking Union Medical College, Beijing, People's Republic of China

\*Email: ksryan@chem.ubc.ca

Contents	Page
Materials and Methods	2
<b>Table S1:</b> Strains and plasmids used in this study	11
<b>Table S2:</b> Primers used in this study	13
<b>Table S3:</b> HR-MS analysis of purified <b>5</b> , <b>1</b> and their derivatives	14
<b>Table S4:</b> Amounts of <b>5</b> -derivatives and <b>1</b> -derivatives obtained	15
<b>Table S5:</b> Substrate scope analysis	15
<b>Figure S1:</b> Cloning genes for <i>in vivo</i> production of <b>1</b> , <b>5</b> and derivatives of <b>5</b>	16
<b>Figure S2:</b> HPLC comparison of <i>E. coli</i> I120 and <i>E. coli</i> I1234670P5	16
<b>Figure S3:</b> LC-MS analysis for synthesis and purification of <b>1</b>	17
<b>Figure S4:</b> UV-vis traces obtained during LC-MS analysis of synthetic steps	17
<b>Figure S5:</b> HPLC analysis of <b>5F-5</b> amounts under different feeding conditions	18
<b>Figure S6:</b> LC-MS analysis of halogen-substituted indole incorporation into <b>5</b>	19
<b>Figure S7:</b> LC-MS analysis of hydroxyindole or azaindole incorporation into <b>5</b>	20
<b>Figure S8:</b> LC-MS analysis of <b>5</b> -derivative esterification	21
<b>Figure S9:</b> LC-MS analysis of <b>7</b> -derivative oxazolinone-cyclizations	22
<b>Figure S10:</b> LC-MS analysis of <b>8</b> -derivative <i>N</i> -methylation	23
<b>Figure S11:</b> Disk diffusion assay of <b>1</b> and its derivatives against MRSA	24
<b>Figure S12:</b> Docking of indolmycin derivatives	25
<b>Figure S13:</b> Predicted tautomeric isomers of indolmycin	26
<b>NMR Spectra</b>	27
<b>References</b>	56

## Materials and Methods

**General methods, materials and strains** Reagents were purchased from Sigma-Aldrich, Thermo Fisher Scientific Canada, New England BioLabs (NEB), Bio-Rad, Bio Basic Inc., Gold Biotechnology, and VWR International. Primers were purchased from Integrated DNA Technologies (IDT). Sequencing was done through the NAPS Unit in the Sequencing and Bioinformatics Consortium at the University of British Columbia.

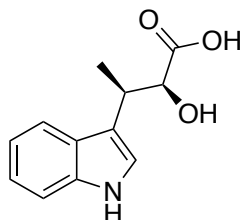
**Cloning** The indolmycin biosynthetic genes (*ind0*, *ind1*, *ind2*, *ind3*, *ind4*, *ind6* and *ind7*) were PCR amplified from *Streptomyces griseus* ATCC 12648 genomic DNA using the primers described in **Table S1**. Genes *ind1*, *ind3* and *ind6* were cloned using into the NcoI and HindIII restriction sites of MCS1 of pETduet-1, pCDFduet-1 and pACYCduet-1, respectively, using Gibson Assembly (NEB). Genes *ind0*, *ind2*, *ind4* and *ind7* were cloned using T4 ligase into MCS2 pCOLAduet-1, *ind1*-pETduet-1, *ind3*-pCDFduet-1 and *ind6*-pACYCduet-1, respectively, using the NdeI and XhoI restriction sites (**Table S2**). The gene *pel5* from *Paenibacillus elgii* B69, was PCR amplified from a pET28a vector containing *pel5* described previously,<sup>1</sup> and was cloned using T4 ligase into the NcoI and HindIII restriction sites of MCS1 in *ind0*-pCOLAduet-1. The *trpS* gene from *Salmonella enterica* was PCR amplified from pSTB7 and cloned using Gibson Assembly into MCS1 of *ind0*-pCOLAduet-1 using the NcoI and HindIII restriction sites, replacing *pel5* for production of indolmycenic acid derivatives. The resulting vectors were transformed into electrocompetent *E. coli* DH5 $\alpha$  by electroporation and selection on LB agar plates containing kanamycin (50  $\mu$ g/mL) for pCOLAduet, ampicillin (100  $\mu$ g/mL) for pETduet, chloramphenicol (34  $\mu$ g/mL) for pACYCduet, or spectinomycin (100  $\mu$ g/mL) for pCDFduet. For co-expression of the genes, the appropriate vectors were co-transformed into electrocompetent *E. coli* BL21 (DE3) by electroporation and successful transformants were selected for on LB plates containing kanamycin (25  $\mu$ g/mL) for pCOLAduet, ampicillin (50  $\mu$ g/mL) for pETduet, chloramphenicol (17  $\mu$ g/mL) for pACYCduet, or spectinomycin (50  $\mu$ g/mL) for pCDFduet. See **Table S2** for description of each type of transformed *E. coli*.

**Expression and feeding** *E. coli* I1234670P5 and I1234670TS were initially grown in 50 mL of LB media containing kanamycin (25  $\mu$ g/mL), ampicillin (50  $\mu$ g/mL), chloramphenicol (17  $\mu$ g/mL) and spectinomycin (50  $\mu$ g/mL) for profiling metabolites, analyzing substrate scopes, and optimizing the feeding procedure. For larger-scale production of IMA and IMA derivatives, *E. coli*

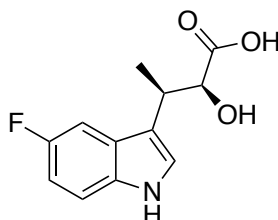
I1234670TS was grown in two 500 mL portions of LB media containing the antibiotics mentioned above. Cultures were allowed to grow until 0.4-0.6 OD<sub>600</sub> at 37 °C with shaking at 200 rpm, after which the temperature and shaking were lowered to 16 °C and 150 rpm, respectively, for 30 min prior to addition of 0.5 mM of isopropyl β-D-1-thiogalactopyranoside (IPTG) to induce expression of the biosynthetic genes. The cultures were incubated for 16 h at 16 °C and 150 rpm. Then, the temperature was raised to 30 °C and the cultures were fed solid indoles or substituted indoles to a final concentration of 0.5 mM in each 500 mL culture once per day for 2 d. Compounds made by the system were harvested 24 h after the final indole feeding. Use of *trpS* for improved acceptance of substituted indoles was tested with 5-fluorindole fed to 1 mM final concentration. Feeding optimization was done with 5-fluoroindole at 0.05 mM to 2 mM final concentration for 1 d, 2 d or 3 d to determine what conditions produced the most 5-fluoro-indolmycenic acid (**Figure S5**).

**Extraction and purification of indolmycenic acid and its derivatives** Cell cultures were adjusted to pH 3-4 with HCl and then extracted with two volumes of ethyl acetate, which was gravity filtered and evaporated under low pressure. To analyze the metabolite profile and substrate scope, the resulting residues from small-scale test cultures were dissolved in 1 mL of methanol and analyzed by LC-MS using a 6120 Quadrupole LC-MS system (Agilent) operated in positive ion mode on an Agilent 5 TC18(2) 250 x 4.6 mm column using 85:15% water:ACN to 5:95% water:ACN (v/v) with 0.1% (v/v) formic acid run at 1 mL/min for 20 min. Quantification of the analogs of compound **5** were assessed by comparing peak integrations of the extracted ion chromatograms for the corresponding *m/z* of each compound with the extracted 220 *m/z* signal for compound **5** from the same sample. Analogues that produced signals greater than 48% of the 220 *m/z* signal (shaded dark blue in **Figure 3b**) were further purified and used in synthetic steps towards **1** (**Table S5**). Initial tests for biosynthetic production of **1** (**Figure 2a**) were analyzed by the same system above, but with a Phenomenex Luna C18(2), 5 μm, 4.6 mm ID × 250 mm column using 95:5% water:ACN to 0:100% water:ACN (v/v) with 0.1% (v/v) formic acid run at 0.6 mL/min for 20 min. When testing the optimal feeding conditions, the metabolites were analyzed by HPLC using a 1260 HPLC apparatus (Agilent) system and an Agilent 5 TC18(2) 250 x 4.6 mm column for the LC-MS analysis. Each metabolite was analyzed using a 75:25% water:ACN to 50:50% water:ACN (v/v) gradient containing 0.1% (v/v) formic acid run at 1 mL/min for 25 min. Testing omission of unnecessary indolmycin genes (**Figure S2**), was done with the HPLC system and column mentioned above but with a gradient of 85%:15% water:ACN to 60%:40% water:ACN

(v/v) with 0.1% (v/v) formic acid run at 1 mL/min for 25 min. The **5F-5** peak eluted at 21.8 min and the area of the peak was used to determine the optimal feeding conditions based on the largest peak area. For large-scale growth, the resulting residue was dissolved in 6-7 mL of methanol for purification via semi-preparative HPLC. Semi-preparative HPLC was run with an 6120 Quadrupole LC-MS system (Agilent) using a Luna C18(2), 5  $\mu\text{m}$ , 250 mm  $\times$  10 mm column (Phenomenex) using a gradient from 70:30% water:ACN (v/v) with 0.1% (v/v) formic acid to 42:58% water:ACN (v/v) at 3.0 mL min<sup>-1</sup> in 12 min. The collected fraction containing the desired peak for **5**, or one of its derivatives, was verified by LC-MS using the conditions described above for analyzing the metabolite profile and substrate scope. **5** and its derivatives were lyophilized and the masses were measured to determine the final amounts obtained. High resolution-mass spectrometry (HR-MS) and nuclear magnetic resonance (NMR) were used to confirm the identity of **5** and its derivatives. HR-MS was done on a Waters/Micromass LCT TOF-MS with electrospray ionization in positive ion mode. NMR analysis was done in dimethyl sulfoxide (DMSO)-*d*<sub>6</sub> with a Bruker Avance 400dir spectrometer.

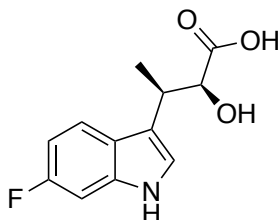


**5**: <sup>1</sup>H NMR (400 MHz, DMSO-*d*<sub>6</sub>)  $\delta$  10.79 (s, 1H), 7.54 (d, *J* = 7.8 Hz, 1H), 7.33 (d, *J* = 8.0 Hz, 1H), 7.14 (d, *J* = 2.4 Hz, 1H), 7.08 – 7.01 (m, 1H), 6.96 (t, *J* = 7.6 Hz, 1H), 4.19 (d, *J* = 4.6 Hz, 1H), 3.42 (qd, *J* = 7.0, 4.4 Hz, 1H), 1.25 (d, *J* = 7.1 Hz, 3H). <sup>13</sup>C NMR (101 MHz, DMSO)  $\delta$  175.26, 136.11, 126.49, 122.40, 120.73, 118.51, 118.14, 116.85, 111.36, 73.99, 34.02, 15.38.

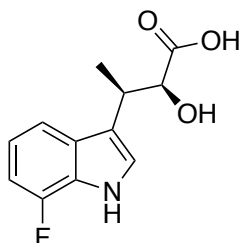


**5F-5**: <sup>1</sup>H NMR (400 MHz, DMSO-*d*<sub>6</sub>)  $\delta$  10.91 (s, 1H), 7.31 (dd, *J* = 8.8, 4.7 Hz, 1H), 7.26 (dd, *J* = 10.3, 2.6 Hz, 1H), 7.22 (d, *J* = 2.5 Hz, 1H), 6.88 (td, *J* = 9.1, 2.6 Hz, 1H), 4.13 (d, *J* = 4.7 Hz, 1H), 3.37 – 3.31 (m, 1H), 1.24 (d, *J* = 7.1 Hz, 3H). <sup>13</sup>C NMR (101 MHz, DMSO-*d*<sub>6</sub>)  $\delta$

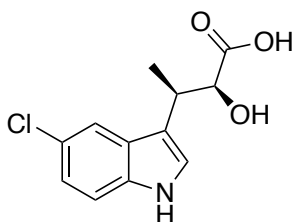
175.14, 156.52 (d,  $J = 230.5$  Hz), 132.77, 126.69 (d,  $J = 9.7$  Hz), 124.63, 117.15 (d,  $J = 4.7$  Hz), 112.20 (d,  $J = 9.7$  Hz), 108.79 (d,  $J = 26.2$  Hz), 103.35 (d,  $J = 23.2$  Hz), 74.12, 34.09, 15.44.



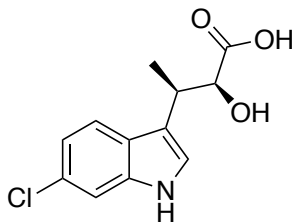
**6F-5:**  $^1\text{H}$  NMR (400 MHz,  $\text{DMSO-}d_6$ )  $\delta$  10.87 (s, 1H), 7.52 (dd,  $J = 8.7, 5.5$  Hz, 1H), 7.16 – 7.05 (m, 2H), 6.82 (ddd,  $J = 9.7, 8.7, 2.4$  Hz, 1H), 4.15 (d,  $J = 4.6$  Hz, 1H), 3.38 (dt,  $J = 12.0, 6.9$  Hz, 1H), 1.23 (d,  $J = 7.1$  Hz, 3H).  $^{13}\text{C}$  NMR (101 MHz,  $\text{DMSO-}d_6$ )  $\delta$  175.16, 158.68 (d,  $J = 233.5$  Hz), 135.88 (d,  $J = 12.6$  Hz), 123.38, 122.99 (d,  $J = 3.4$  Hz), 119.53 (d,  $J = 10.3$  Hz), 117.13, 106.55 (d,  $J = 24.4$  Hz), 97.20 (d,  $J = 25.4$  Hz), 74.02, 34.01, 15.36.



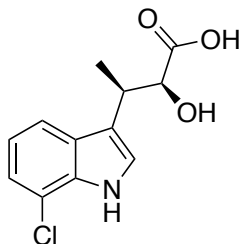
**7F-5:**  $^1\text{H}$  NMR (400 MHz,  $\text{DMSO-}d_6$ )  $\delta$  11.30 (s, 1H), 7.36 (d,  $J = 7.8$  Hz, 1H), 7.20 (d,  $J = 2.4$  Hz, 1H), 6.98 – 6.83 (m, 2H), 4.17 (d,  $J = 4.6$  Hz, 1H), 3.41 (qd,  $J = 7.0, 4.4$  Hz, 1H), 1.25 (d,  $J = 7.1$  Hz, 3H).  $^{13}\text{C}$  NMR (101 MHz,  $\text{DMSO-}d_6$ )  $\delta$  175.13, 149.31 (d,  $J = 242.4$  Hz), 130.61 (d,  $J = 6.0$  Hz), 123.80 (d,  $J = 13.0$  Hz), 123.66, 118.47 (d,  $J = 6.1$  Hz), 118.07 (d,  $J = 2.0$  Hz), 114.83 (d,  $J = 3.3$  Hz), 105.56 (d,  $J = 15.9$  Hz), 73.89, 34.07, 15.37.



**5Cl-5:**  $^1\text{H}$  NMR (400 MHz,  $\text{DMSO-}d_6$ )  $\delta$  11.01 (s, 1H), 7.55 (d,  $J = 2.0$  Hz, 1H), 7.34 (d,  $J = 8.6$  Hz, 1H), 7.21 (d,  $J = 2.3$  Hz, 1H), 7.04 (dd,  $J = 8.6, 2.1$  Hz, 1H), 4.08 (d,  $J = 4.3$  Hz, 1H), 3.40 – 3.33 (m, 1H), 1.21 (d,  $J = 7.1$  Hz, 3H).  $^{13}\text{C}$  NMR (101 MHz,  $\text{DMSO-}d_6$ )  $\delta$  175.29, 134.65, 127.75, 124.44, 122.91, 120.71, 118.05, 117.22, 112.95, 74.29, 34.03, 15.35.



**6Cl-5:**  $^1\text{H}$  NMR (400 MHz,  $\text{DMSO-}d_6$ )  $\delta$  10.95 (s, 1H), 7.54 (d,  $J = 8.5$  Hz, 1H), 7.36 (d,  $J = 1.9$  Hz, 1H), 7.18 (d,  $J = 2.3$  Hz, 1H), 6.97 (dd,  $J = 8.4, 1.9$  Hz, 1H), 4.12 (d,  $J = 4.5$  Hz, 1H), 3.39 (qd,  $J = 7.0, 4.2$  Hz, 1H), 1.23 (d,  $J = 7.1$  Hz, 3H).  $^{13}\text{C}$  NMR (101 MHz,  $\text{DMSO-}d_6$ )  $\delta$  175.76, 137.06, 126.05, 125.94, 124.19, 120.59, 119.04, 117.95, 111.50, 74.66, 34.54, 15.91.



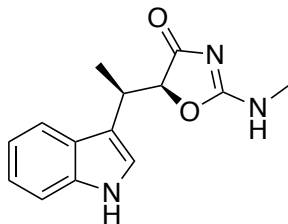
**7Cl-5:**  $^1\text{H}$  NMR (400 MHz,  $\text{DMSO-}d_6$ )  $\delta$  11.17 (s, 1H), 7.52 (d,  $J = 7.9$  Hz, 1H), 7.21 (d,  $J = 2.5$  Hz, 1H), 7.13 (d,  $J = 7.6$  Hz, 1H), 6.98 (t,  $J = 7.8$  Hz, 1H), 4.16 (d,  $J = 4.6$  Hz, 1H), 3.41 (dt,  $J = 7.1, 3.8$  Hz, 1H), 1.25 (d,  $J = 7.1$  Hz, 3H).  $^{13}\text{C}$  NMR (101 MHz,  $\text{DMSO-}d_6$ )  $\delta$  175.10, 132.82, 128.53, 123.82, 120.28, 119.26, 118.33, 117.73, 115.81, 73.97, 34.09, 15.44.

**Synthesis of indolmycin and its derivatives** The synthetic method for making **1** and its derivatives from **5** and its derivatives was adapted from literature methods to make **1**.<sup>2,3</sup> To form the indolmycenic acid ethyl ester (**7**), or one of its derivatives, 85  $\mu\text{L}$  of acetyl chloride was mixed into 300  $\mu\text{L}$  of ethanol on ice for 30 min. 9-20 mg of **5**, or one of its derivatives, was dissolved in 200  $\mu\text{L}$  of ethanol and added slowly to the acetyl chloride and ethanol mixture over 2-3 min. The resulting mixture was then stirred at room temperature for 6 h. The solvent was rotary evaporated and the resulting residue was dissolved in 400  $\mu\text{L}$  ethyl acetate, washed with 280  $\mu\text{L}$  saturated sodium bicarbonate and 225  $\mu\text{L}$  of brine, and then dried over anhydrous sodium sulfate before the solvent was speed vacuumed, leaving a residue of **7**, or one of its derivatives.

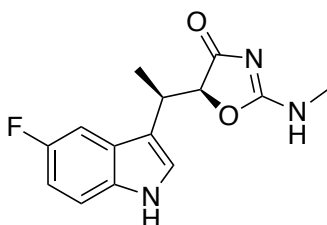
The oxazolinone ring was cyclized to form *N*-desmethyl-indolmycin (**8**), or one of its derivatives, using 20 mg of guanidine, 20 mg of molecular sieves 3Å, and 240  $\mu\text{L}$  of potassium *tert*-butoxide (1 M in THF), which were mixed with 80  $\mu\text{L}$  *tert*-butanol at room temperature for 3 d. The residue of **7**, or one of its derivatives, from the esterification step was dissolved in 160  $\mu\text{L}$  of *tert*-butanol (also dried with sieves for 3 d for derivatives, but not for initial synthesis **1**) and

added to the guanidine/sieves/potassium *tert*-butoxide mixture, which was then stirred for 7.5 h at room temperature. The reaction was stopped with the addition of 800  $\mu\text{L}$  of cold, saturated ammonium chloride. The liquids partitioned into two layers, which were separated from each other after centrifugation. The aqueous ammonium chloride layer was washed with 500  $\mu\text{L}$  of ethyl acetate, which was combined with the organic layer. Then the organic layer was washed with 200  $\mu\text{L}$  of 5% sodium bicarbonate and dried with anhydrous sodium sulfate before the solvent was speed vacuumed, leaving a residue of **8**, or one of its derivatives.

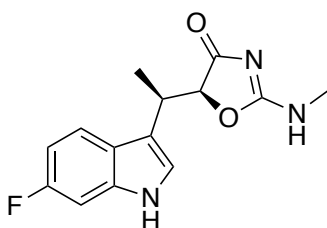
Compound **1** and its derivatives were formed by *N*-methylating **8** and derivatives of **8** obtained from the previous reaction. Compound **8**, or one of its derivatives, was dissolved in 65  $\mu\text{L}$  of 40% (w/v) methylamine and incubated at 4°C for 5 h. The solvent was evaporated by speed vacuum and the resulting residue was dissolved in 500  $\mu\text{L}$  of methanol for purification by semi-preparative HPLC, as described above for the purification of **5** and its derivatives. To further purify **1** from residual **5** after an initial semi-preparative HPLC purification, semi-preparative HPLC was run again, but at 48%:52% to 54%:46% ACN:water (v/v) with 0.1% (v/v) formic acid over 12 min. Fractions containing **1**, or one of its derivatives, were verified by LC-MS and lyophilized to measure the final mass and determine the amount obtained. We attribute the low yield for underivatized **1** to a high amount of **5** regenerated in the oxazolinone-cyclization step to generate compound **8** (**Figure S5**). Compound **1** and its derivatives were characterized by HR-MS and NMR to confirm their identity. HR-MS was done on a Waters/Micromass LCT TOF-MS with electrospray ionization in positive ion mode. NMR analysis was done in DMSO- $d_6$  with a Bruker Avance 600 MHz spectrometer or a Bruker Avance 400dir spectrometer. Tautomeric isomers of **1** and its derivatives were observed in a 2:1 ratio, favouring the natural isomer, from all the NMR spectra (**Figure S13**), so a varied temperature NMR experiment was done on **5F-1** between 25°C and 115°C with a Bruker Avance 400inv spectrometer. Observation of these isomers has been reported previously.<sup>2-4</sup>



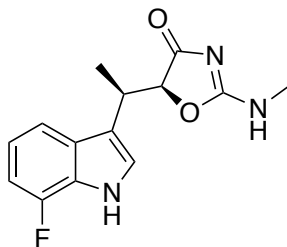
**1:**  $^1\text{H}$  NMR (400 MHz,  $\text{DMSO-}d_6$ )  $\delta$  10.91 (s, 1H), 8.75 (s, 1/3H), 8.68 – 8.60 (m, 2/3H), 7.58 (dd,  $J = 8.0, 4.3$  Hz, 1H), 7.35 (d,  $J = 8.1$  Hz, 1H), 7.18 (d,  $J = 2.4$  Hz, 1/3H), 7.15 (d,  $J = 2.4$  Hz, 2/3H), 7.08 (ddt,  $J = 9.1, 7.8, 1.7$  Hz, 1H), 6.99 (t,  $J = 7.4$  Hz, 1H), 4.94 (d,  $J = 2.6$  Hz, 2/3H), 4.91 (d,  $J = 2.7$  Hz, 1/3H), 3.66 – 3.51 (m, 1H), 2.80 (d,  $J = 4.5$  Hz, 2H), 2.77 (s, 1H), 1.25 (d,  $J = 7.3$  Hz, 1H), 1.19 (d,  $J = 7.1$  Hz, 2H).  $^{13}\text{C}$  NMR (101 MHz,  $\text{DMSO-}d_6$ )  $\delta$  186.59, 175.68, 136.20, 126.07, 122.44, 121.01, 118.52, 118.46, 115.32, 111.46, 85.35, 31.69, 28.81, 13.56.



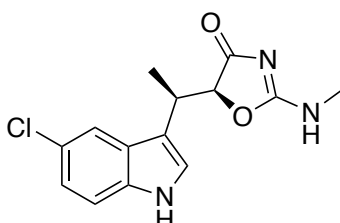
**5F-1:**  $^1\text{H}$  NMR (400 MHz,  $\text{DMSO-}d_6$ )  $\delta$  11.02 (d,  $J = 3.1$  Hz, 1H), 8.70 (s, 1/3H), 8.67 – 8.59 (m, 2/3H), 7.38 – 7.19 (m, 3H), 6.96 – 6.85 (m, 1H), 4.93 (d,  $J = 2.7$  Hz, 2/3H), 4.90 (d,  $J = 2.8$  Hz, 1/3H), 3.63 – 3.47 (m, 1H), 2.79 (d,  $J = 4.4$  Hz, 2H), 2.77 (s, 1H), 1.25 (d,  $J = 7.2$  Hz, 1H), 1.19 (d,  $J = 7.2$  Hz, 2H).  $^{13}\text{C}$  NMR (101 MHz,  $\text{DMSO-}d_6$ )  $\delta$  187.28, 176.33, 157.27 (d,  $J = 230.8$  Hz), 133.42 (d,  $J = 8.2$  Hz), 126.92 (d,  $J = 9.8$  Hz), 125.24, 116.18 (d,  $J = 4.9$  Hz), 112.97 (d,  $J = 9.6$  Hz), 109.75 (d,  $J = 26.1$  Hz), 104.02 (d,  $J = 23.4$  Hz), 85.84, 32.29, 29.42, 14.32.



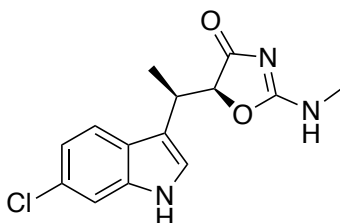
**6F-1:**  $^1\text{H}$  NMR (600 MHz,  $\text{DMSO-}d_6$ )  $\delta$  10.97 (s, 1H), 8.69 (s, 1/3H), 8.64 – 8.59 (m, 2/3H), 7.57 – 7.51 (m, 1H), 7.18 – 7.05 (m, 2H), 6.85 – 6.77 (m, 1H), 4.89 (d,  $J = 2.7$  Hz, 2/3H), 4.86 (d,  $J = 2.8$  Hz, 1/3H), 3.60 – 3.48 (m, 1H), 2.76 (d,  $J = 4.7$  Hz, 2H), 2.73 (d,  $J = 4.1$  Hz, 1H), 1.20 (d,  $J = 7.2$  Hz, 1H), 1.14 (d,  $J = 7.0$  Hz, 2H).  $^{13}\text{C}$  NMR (151 MHz,  $\text{DMSO-}d_6$ )  $\delta$  186.67, 175.76, 158.79 (d,  $J = 234.0$  Hz), 136.04 (d,  $J = 12.7$  Hz), 123.09 (d,  $J = 3.3$  Hz), 122.98, 119.68 (d,  $J = 10.1$  Hz), 115.58, 106.91 (d,  $J = 24.3$  Hz), 97.36 (d,  $J = 25.3$  Hz), 85.25, 31.67, 28.83, 13.62.



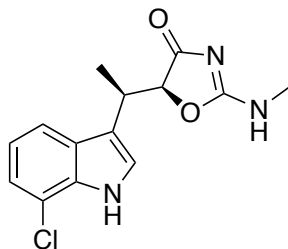
**7F-1:**  $^1\text{H}$  NMR (600 MHz,  $\text{DMSO-}d_6$ )  $\delta$  11.44 (s, 1H), 8.73 (s, 1/3H), 8.68 – 8.64 (m, 2/3H), 7.46 – 7.32 (m, 1H), 7.27 – 7.14 (m, 1H), 7.01 – 6.88 (m, 2H), 4.94 (d,  $J = 2.6$  Hz, 2/3H), 4.90 (d,  $J = 2.8$  Hz, 1/3H), 3.65 – 3.51 (m, 1H), 2.79 (d,  $J = 4.6$  Hz, 2H), 2.76 (s, 1H), 1.25 (d,  $J = 7.2$  Hz, 1H), 1.18 (d,  $J = 7.1$  Hz, 2H).  $^{13}\text{C}$  NMR (151 MHz,  $\text{DMSO-}d_6$ )  $\delta$  186.64, 175.77, 149.25 (d,  $J = 242.6$  Hz), 130.15 (d,  $J = 5.7$  Hz), 123.85 (d,  $J = 19.9$  Hz), 123.69, 118.83 (d,  $J = 6.2$  Hz), 116.56, 114.92, 105.88 (d,  $J = 16.0$  Hz), 85.16, 31.71, 28.84, 13.67.



**5Cl-1:**  $^1\text{H}$  NMR (600 MHz,  $\text{DMSO-}d_6$ )  $\delta$  11.14 (s, 1H), 8.70 (s, 1/3H), 8.67 – 8.62 (m, 2/3H), 7.64 – 7.57 (m, 1H), 7.39 – 7.31 (m, 1H), 7.27 – 7.20 (m, 1H), 7.10 – 7.01 (m, 1H), 4.94 (d,  $J = 2.8$  Hz, 2/3H), 4.89 (d,  $J = 2.8$  Hz, 1/3H), 3.64 – 3.51 (m, 1H), 2.81 – 2.76 (m, 3H), 1.27 (d,  $J = 7.2$  Hz, 1H), 1.18 (d,  $J = 7.1$  Hz, 2H).  $^{13}\text{C}$  NMR (151 MHz,  $\text{DMSO-}d_6$ )  $\delta$  186.66, 175.72, 134.62, 127.24, 124.42, 123.23, 121.02, 117.82, 115.21, 113.01, 85.13, 31.51, 28.84, 13.76.



**6Cl-1:**  $^1\text{H}$  NMR (400 MHz,  $\text{DMSO-}d_6$ )  $\delta$  11.07 (s, 1H), 8.70 (s, 1/3H), 8.65 – 8.59 (m, 2/3H), 7.64 – 7.51 (m, 1H), 7.42 – 7.30 (m, 1H), 7.25 – 7.10 (m, 1H), 7.04 – 6.91 (m, 1H), 4.92 (d,  $J = 2.7$  Hz, 2/3H), 4.89 (d,  $J = 3.0$  Hz, 1/3H), 3.63 – 3.48 (m, 1H), 2.78 (d,  $J = 4.1$  Hz, 2H), 2.76 (s, 1H), 1.25 (d,  $J = 7.2$  Hz, 1H), 1.19 (d,  $J = 7.1$  Hz, 2H).  $^{13}\text{C}$  NMR (101 MHz,  $\text{DMSO-}d_6$ )  $\delta$  186.58, 175.71, 136.56, 125.74, 124.93, 123.65, 120.06, 118.75, 115.60, 111.02, 85.17, 31.60, 28.80, 13.63.



**7Cl-1:**  $^1\text{H}$  NMR (400 MHz,  $\text{DMSO-}d_6$ )  $\delta$  11.30 (s, 1H), 8.69 – 8.63 (m, 1H), 7.62 – 7.50 (m, 1H), 7.26 – 7.09 (m, 2H), 7.05 – 6.95 (m, 1H), 4.94 (d,  $J = 2.7$  Hz, 2/3H), 4.91 (d,  $J = 2.8$  Hz, 1/3H), 3.67 – 3.48 (m, 1H), 2.79 (d,  $J = 4.2$  Hz, 2H), 2.75 (s, 1H), 1.27 (d,  $J = 7.2$  Hz, 1H), 1.19 (d,  $J = 7.2$  Hz, 2H).  $^{13}\text{C}$  NMR (101 MHz,  $\text{DMSO-}d_6$ )  $\delta$  186.59, 175.73, 132.92, 128.12, 123.81, 120.58, 119.55, 117.81, 116.78, 115.85, 85.14, 31.70, 28.82, 13.81.

**Biological Analysis** Disk diffusion assays were done on Mueller-Hinton Agar plates with MRSA (*Staphylococcus aureus* ATCC 33591). Each derivative was dissolved in water with 0.5% DMSO and deposited on the disks. Rifampicin (1  $\mu\text{g}$ ) was used as a positive control and 0.5% DMSO was used as a negative control. Each disk contained either 10  $\mu\text{g}$  of **1**, 20  $\mu\text{g}$  of **6F-1** or **7F-1**, or 30  $\mu\text{g}$  of **5F-1**, **5Cl-1**, **6Cl-1**, or **7Cl-1** and was deposited onto the petri dishes containing a lawn of the MRSA culture. The petri dishes were allowed to grow overnight, after which zones of inhibition were visible. The minimum inhibitory concentration (MIC) measurements were done by diluting an overnight culture of *S. aureus* ATCC 33591 to  $\sim 1 \times 10^5$  cells/mL with Mueller-Hinton Broth (MHB). Various dilutions of **1** and its derivatives and the positive control, rifampicin, were prepared. Rifampicin is a broad spectrum antibiotic with a known  $\text{MIC}_{50}$  activity of 0.008  $\mu\text{g/mL}$  (range: 0.004 – 0.5  $\mu\text{g/mL}$ ) against MRSA.<sup>5</sup> DMSO was used as a negative control. Concentrations ranged from 50  $\mu\text{g/mL}$  to 0.128  $\text{ng/mL}$  for **1**, **5F-1**, **6F-1** and **7F-1** and from 200  $\mu\text{g/mL}$  to 0.512  $\text{ng/mL}$  for **5Cl-1**, **6Cl-1** and **7Cl-1**. The rifampicin sample concentrations ranged from 10  $\mu\text{g/mL}$  to 0.0256  $\text{ng/mL}$ . The 100  $\mu\text{L}$  of *S. aureus* cells and 10  $\mu\text{L}$  of each diluted sample were combined in a 96-well plate and diluted to 200  $\mu\text{L}$  with 90  $\mu\text{L}$  MHB. Each sample concentration for each compound was tested in triplicate. The 96-well plate was covered and incubated at 37°C for 18 h before measuring the OD at 600 nm using a Molecular Devices FilterMax F5 Multi-Mode Microplate Reader. Readings from blank samples were subtracted from each sample reading to remove background signal and the percent of cells alive was calculated in comparison to the DMSO negative control. The  $\text{MIC}_{50}$  values were determined from the percent alive using the Quest Graph IC50 Calculator online tool from AAT Bioquest.<sup>6</sup> The  $\text{MIC}_{50}$  value determined for

rifampicin, the positive control, was  $0.0047 \pm 0.0013 \mu\text{g/mL}$ . Docking experiments to test analog binding to a TrpRS was done using AutoDock Vina<sup>7</sup> and the structures for **1** and its derivatives were generated using Phenix eLBOW.<sup>8</sup> The TrpRS model used for docking was from *Bacillus stearothermophilus* (PDB: 5DK4) and the cocrystallized ligands, ATP, Mg<sup>2+</sup> and indolmycin, were removed from the model before docking.

**Table S1:** Strains and plasmids used in this study.

Name	Description	Source
<b>Strains</b>		
<i>E. coli</i> DH5 $\alpha$	General cloning host	Laboratory stock
<i>E. coli</i> BL21 (DE3)	Host for protein expression	Laboratory stock
<i>Streptomyces griseus</i> ATCC 12648	Wild-type indolmycin producer	ATCC
<i>E. coli</i> I120	<i>E. coli</i> carrying pI0COLA and pI1I2ET; tested for <i>in vivo</i> production of indolmycenic acid	This study
<i>E. coli</i> I1234670P5	<i>E. coli</i> carrying pP5I0COLA, pI1I2ET, pI3I4CDF and pI6I7ACYC; used for <i>in vivo</i> production of indolmycin	This study
<i>E. coli</i> I1234670TS	<i>E. coli</i> carrying pT5I0COLA, pI1I2ET, pI3I4CDF and pI6I7ACYC; used for <i>in vivo</i> production of IMA and IMA derivatives	This study
<i>Staphylococcus aureus</i> ATCC 33591	Methicillin resistant strain of <i>S. aureus</i> for bioactivity testing	ATCC
<b>Plasmids</b>		
pCOLAduet-1	Vector for protein expression in <i>E. coli</i> with two multiple cloning sites	Laboratory stock

pETduet-1	Vector for protein expression in <i>E. coli</i> with two multiple cloning sites	Laboratory stock
pCDFduet-1	Vector for protein expression in <i>E. coli</i> with two multiple cloning sites	Laboratory stock
pACYCduet-1	Vector for protein expression in <i>E. coli</i> with two multiple cloning sites	Laboratory stock
pET28a- <i>pel5</i>	Template for <i>pel5</i> amplification	Du <i>et al.</i> <sup>1</sup>
pSTB7 (ATCC 37845)	Vector carrying <i>trpS</i> from <i>Salmonella enterica</i>	ATCC
pI0COLA	Vector for cloning <i>pel5</i> and <i>trpS</i>	This study
pI1ET	Vector for cloning <i>ind2</i>	This study
pI3CDF	Vector for cloning <i>ind4</i>	This study
pI6ACYC	Vector for cloning <i>ind7</i>	This study
pP5I0COLA	Vector for <i>ind0</i> and <i>pel5</i> expression	This study
pI1I2ET	Vector for <i>ind1</i> and <i>ind2</i> expression	This study
pI3I4CDF	Vector for <i>ind3</i> and <i>ind4</i> expression	This study
pI6I7ACYC	Vector for <i>ind6</i> and <i>ind7</i> expression	This study
pTSI0COLA	Vector for <i>ind0</i> and <i>trpS</i> expression	This study

**Table S2:** Primers used in this study

Primer Name	Sequence (5' to 3')	Description
Ind0_F	ATTAGTTAAGTATAAGAAGGAGATATA CATATGATCAAGCTGTCCGGAATCACCC	Cloning <i>ind0</i> into pCOLAduet-1
Ind0_R	CGGTTTCTTTACCAGACTCGAGTCAGCC CACTCCGGCGAGTT	Cloning <i>ind0</i> into pCOLAduet-1
NcoI-Pel5-F	ACTTTAATAAGGAGATATACCATGGATG AGAATCATTTATCTGGATCAACCTACCT AC	Cloning <i>pel5</i> into pI0COLA
HindIII-Pel5-R	CTTAAGCATTATGCGGCCGCAAGCTTTC ATTCGCTTGCCGGCCTCTTC	Cloning <i>pel5</i> into pI0COLA
pCOLA-TrpS-F	TAATTTTGTTTAACTTTAATAAGGAGAT ATACATGACAACACTTCTCAACCCCTAC TTTG	Cloning <i>trpS</i> into pI0COLA
pCOLA-TrpS-R	ATTATGCGGCCGCAAGCTTTATGCGCGG CTGGCGGC	Cloning <i>trpS</i> into pI0COLA
Ind1-3_F	AACTTTAAGAAGGAGATATACCATGAC CAGGACCGATTTCGCC	Cloning <i>ind1</i> into pETduet-1
Ind1-HindIII-R	GCATTATGCGGCCGCAAGCTTCATGAAG CCGGCCC	Cloning <i>ind1</i> into pETduet-1
NdeI-Ind2-F	TAGTTAAGTATAAGAAGGAGATATACA TATGAAGCTGGACGACAAGAGAATTCT C	Cloning <i>ind2</i> into pI1ET
Ind2-XhoI-R	GTTTCTTTACCAGACTCGAGTCATAGGC CCTTGATGCGACGGG	Cloning <i>ind2</i> into pI1ET
Ind3-F	TGTTTAACTTTAATAAGGAGATATACCA TGAAGGGTGCAGACAGGAG	Cloning <i>ind3</i> into pCDFduet-1
Ind3-HindIII-R	GCATTATGCGGCCGCAAGCTTTACGGGA CCAGGCTGATGATCTGGTTG	Cloning <i>ind3</i> into pCDFduet-1
NdeI-Ind4-F2	GTTAAGTATAAGAAGGAGATATACATA TGGAACGGTTCAACAATCTGACG	Cloning <i>ind4</i> into pI3CDF
Ind4-XhoI-R2	GTTTCTTTACCAGACTCGAGTCATGAAC CGGCGCCCTCG	Cloning <i>ind4</i> into pI3CDF
Ind6-F	TGTTTAACTTTAATAAGGAGATATACCA TGTCGTTTCGATAACCAGAACAGG	Cloning <i>ind6</i> into pACYCduet-1
Ind6-HindIII-R	GCATTATGCGGCCGCAAGCTTCAGCCGA CTCCGATGTCTCCAGTC	Cloning <i>ind6</i> into pACYCduet-1
NdeI-Ind7-F	GTTAAGTATAAGAAGGAGATATACATA TGCACACGGACTGGGAGAC	Cloning <i>ind7</i> into pI6ACYC
Ind7-XhoI-R	GTTTCTTTACCAGACTCGAGTCAGGCTG TTCCGCGCAC	Cloning <i>ind7</i> into pI6ACYC
pET Upstream	ATGCGTCCGGCGTAGA	Sequencing <i>ind1</i> in pI1ET
pACYCduetUP1	GGATCTCGACGCTCTCCCT	Sequencing <i>trpS</i> in pTSI0COLA, <i>pel5</i> in

		pP5I0COLA, <i>ind3</i> in pI3CDF, <i>ind6</i> in pI6ACYC
DuetDOWN1	GATTATGCGGCCGTGTACAA	Sequencing <i>trpS</i> in pTSI0COLA, <i>ind1</i> in pI1ET, <i>ind3</i> in pI3CDF, <i>ind6</i> in pI6ACYC
DuetUP2	TTGTACACGGCCGCATAATC	Sequencing <i>ind0</i> in pI0COLA, <i>ind2</i> in pI1I2ET, <i>ind4</i> in pI3I4CDF, <i>ind7</i> in pI6I7CYC
T7-term	GCTAGTTATTGCTCAGCGG	T7 terminator for sequencing <i>ind0</i> in pI0COLA, <i>ind2</i> in pI1I2ET, <i>ind4</i> in pI3I4CDF, <i>ind7</i> in pI6I7ACYC
TrpS-seq-F1	GCTCAAACGCTATCGGGATGTTTG	Sequencing <i>trpS</i> in pTSI0COLA
TrpS-seq-F2	GTACGCGAATCTGGTGTTCATAACG	Sequencing <i>trpS</i> in pTSI0COLA
TrpS-seq-R1	CCATATAGATACGGCATTTCAGACCCAG	Sequencing <i>trpS</i> in pTSI0COLA
TrpS-seq-R2	CGTAGCGTTCATCAGATTTCCCC	Sequencing <i>trpS</i> in pTSI0COLA

**Table S3:** HR-MS analysis of purified **5**, **1** and their derivatives.

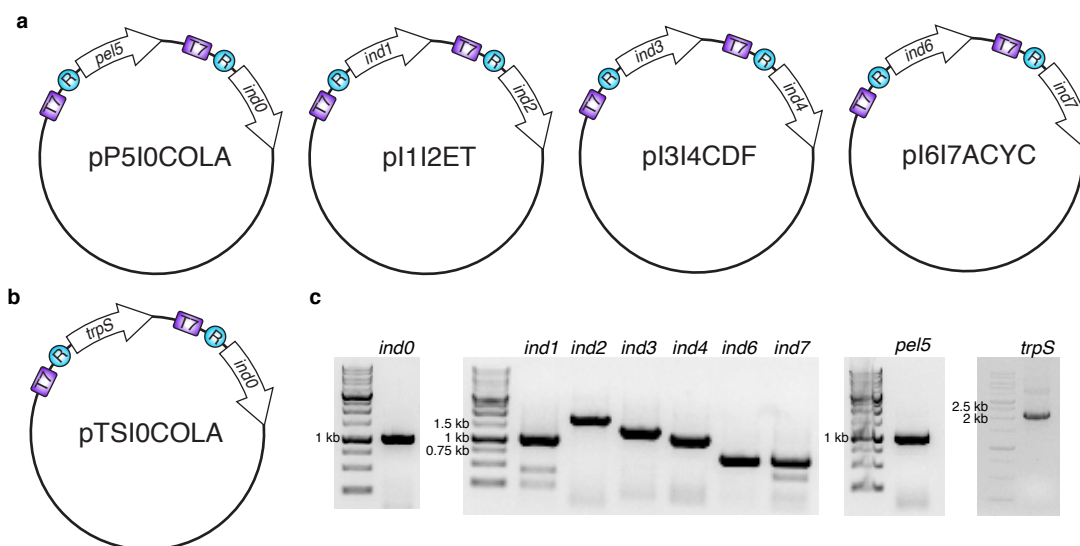
	Observed Mass ( <i>m/z</i> )	Calculated Mass ( <i>m/z</i> )	Chemical Formula	Error (ppm)
IMA	219.0906	219.0895	C <sub>12</sub> H <sub>13</sub> NO <sub>3</sub>	-5
IM	257.1167	257.1164	C <sub>14</sub> H <sub>15</sub> N <sub>3</sub> O <sub>2</sub>	-1
5F-IMA	237.0808	237.0801	C <sub>12</sub> H <sub>12</sub> FNO <sub>3</sub>	-3
5F-IM	275.1082	275.1070	C <sub>14</sub> H <sub>14</sub> FN <sub>3</sub> O <sub>2</sub>	-5
6F-IMA	237.0809	237.0801	C <sub>12</sub> H <sub>12</sub> FNO <sub>3</sub>	-3
6F-IM	275.1078	275.1070	C <sub>14</sub> H <sub>14</sub> FN <sub>3</sub> O <sub>2</sub>	-3
7F-IMA	237.0811	237.0801	C <sub>12</sub> H <sub>12</sub> FNO <sub>3</sub>	-4
7F-IM	275.1076	275.1070	C <sub>14</sub> H <sub>14</sub> FN <sub>3</sub> O <sub>2</sub>	-2
5Cl-IMA	253.0514	253.0506	C <sub>12</sub> H <sub>12</sub> ClNO <sub>3</sub>	-3
5Cl-IM	291.0777	291.0775	C <sub>14</sub> H <sub>14</sub> ClN <sub>3</sub> O <sub>2</sub>	-1
6Cl-IMA	253.0504	253.0506	C <sub>12</sub> H <sub>12</sub> ClNO <sub>3</sub>	-1
6Cl-IM	291.0784	291.0075	C <sub>14</sub> H <sub>14</sub> ClN <sub>3</sub> O <sub>2</sub>	-3
7Cl-IMA	253.0504	253.0506	C <sub>12</sub> H <sub>12</sub> ClNO <sub>3</sub>	-1
7Cl-IM	291.0785	291.0075	C <sub>14</sub> H <sub>14</sub> ClN <sub>3</sub> O <sub>2</sub>	-3

**Table S4:** Amounts of **5**-derivatives and **1**-derivatives obtained. Yields given are for synthetic steps from **5** only. Amounts of **5** are from 1 L of bacterial culture. Low yield for underivatized **1** from indole is attributed to the solvent drying method during production of **8**.

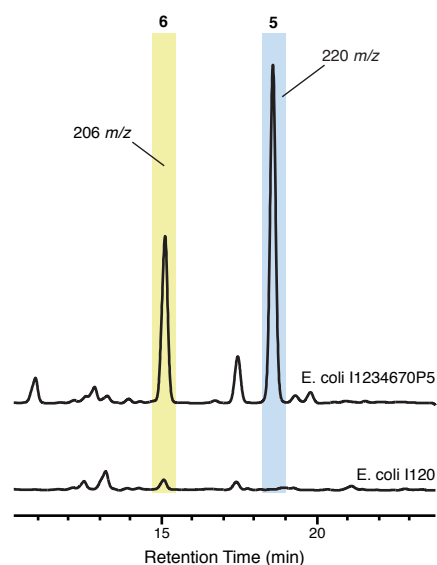
	<b>5</b> and derivatives (mg)	<b>1</b> and derivatives (mg)	% yield
indole	44.1	2.6	5.0
5-fluoroindole	26.9	7.8	25
6-fluoroindole	15.1	2.6	15
7-fluoroindole	24.9	3.1	11
5-chloroindole	9.1	1.7	16
6-chloroindole	10.3	3.3	28
7-chloroindole	10.5	2.6	22

**Table S5:** Substrate scope analysis. Approximate amounts of derivatives of **5** are given as a percentage of underivatized **5** detected in the same sample from LC-MS extracted ion chromatograms at the corresponding  $m/z$  for each compound.

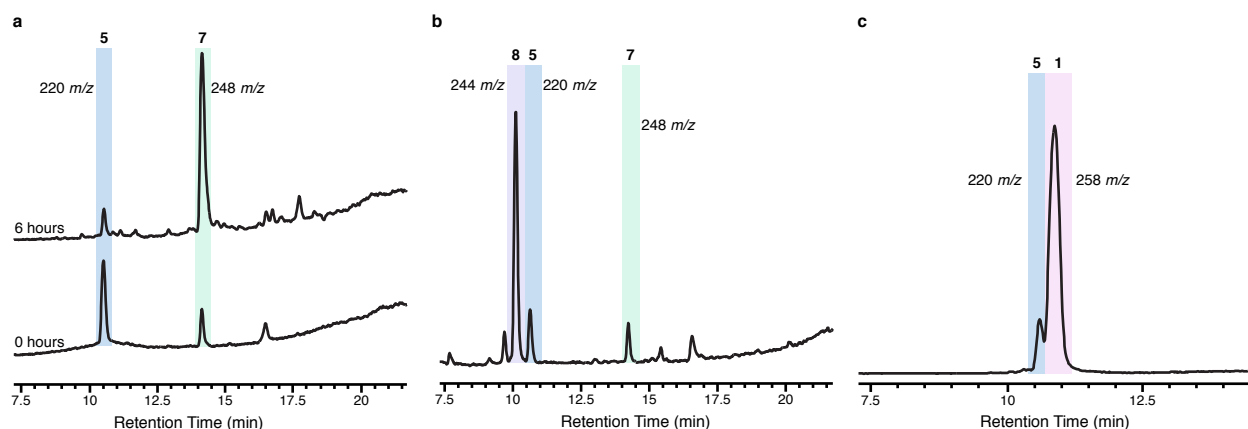
Indole fed to <i>E. coli</i> I1234670TS	$m/z$ for <b>5</b> -derivative	% of <b>5</b>
4-fluoroindole	238	22
5-fluoroindole	238	96
6-fluoroindole	238	55
7-fluoroindole	238	94
4-chloroindole	254/256	0
5-chloroindole	254/256	48
6-chloroindole	254/256	223
7-chloroindole	254/256	65
5-bromoindole	298/300	10
4-azaindole	221	0
5-azaindole	221	0
6-azaindole	221	0
7-azaindole	221	15
4-hydroxyindole	236	0
5-hydroxyindole	236	10
6-hydroxyindole	236	6



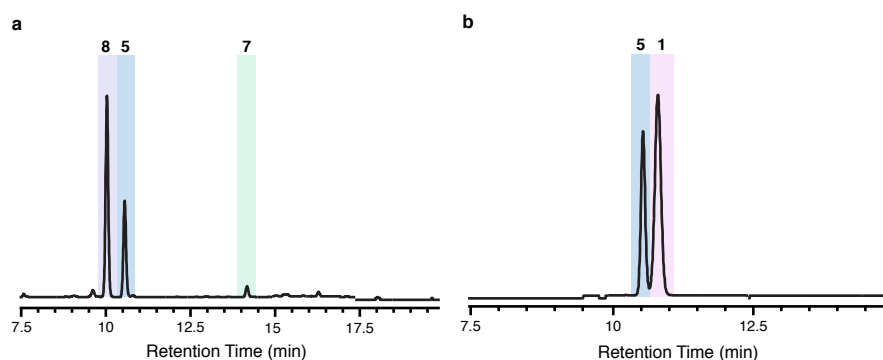
**Figure S1:** Cloning genes for *in vivo* production of **1**, **5** and derivatives of **5**. (a) Plasmids made and used in *E. coli* I1234670P5 to make **1** *in vivo*. (b) Plasmid used in *E. coli* I1234670TS to replace pP510COLA from *E. coli* I1234670P5 for production of **5** and its derivatives. (c) Agarose gels of PCR amplifications for each gene cloned into each of the five plasmids. Expected sizes for each gene are *ind0*: 1018 base pairs; *ind1*: 1032 base pairs; *ind2*: 1761 base pairs; *ind3*: 1406 base pairs; *ind4*: 1198 base pairs; *ind6*: 737 base pairs; *ind7*: 760 base pairs; *pel5*: 1011 base pairs; *trpS*: 2050 base pairs.



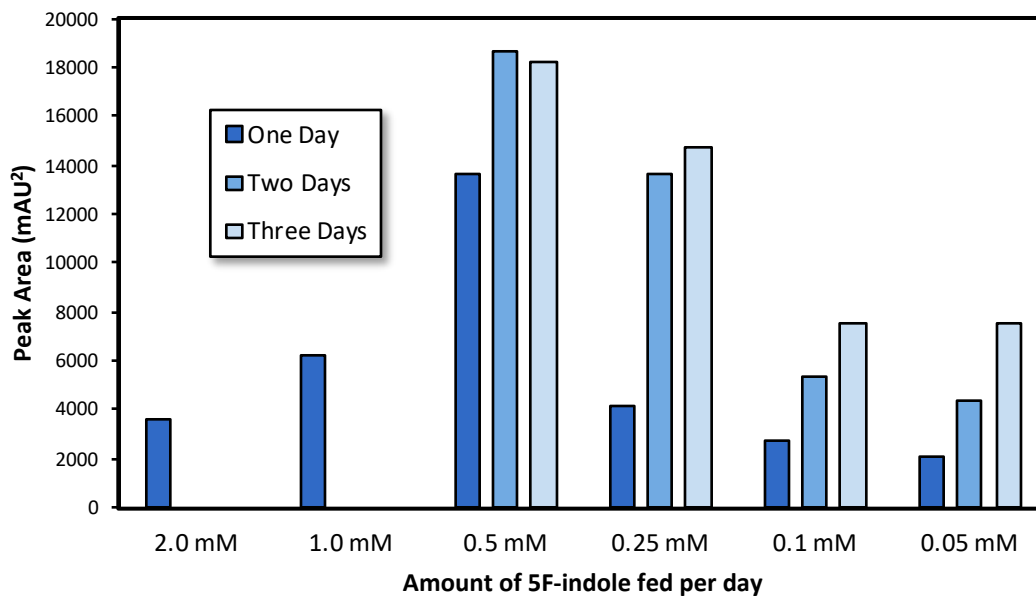
**Figure S2:** HPLC comparison of *E. coli* I120 and *E. coli* I1234670P5 metabolites to understand the effect of removing genes presumably not needed for production of **5**. Relevant peaks identified as indolmycin pathway metabolites are indicated with a coloured box, compound number and their corresponding ion mass from LC-MS analysis. Peaks of relevant compounds have different retention times than other traces of the same compounds because different column chromatography conditions were used.



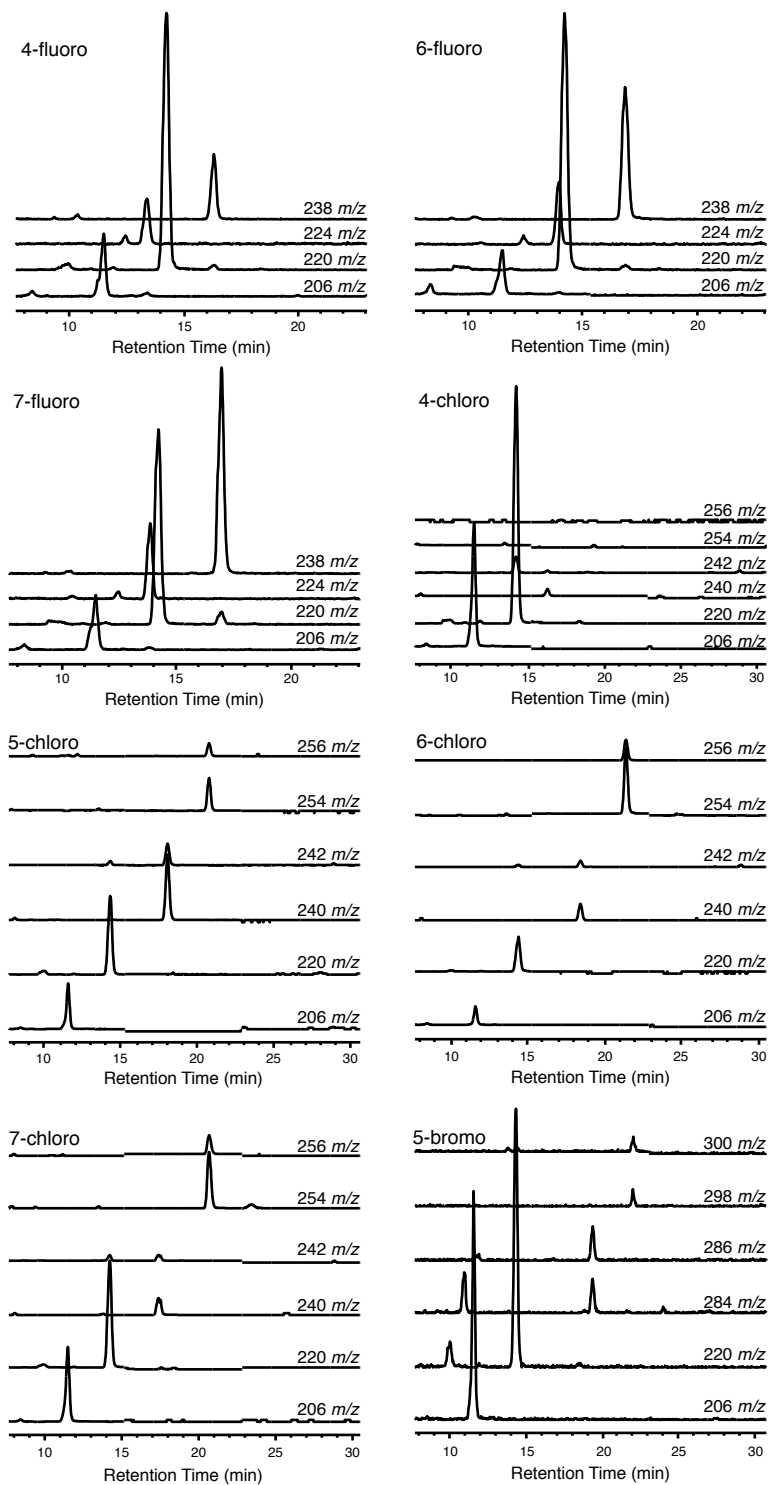
**Figure S3:** LC-MS analysis for synthesis and purification of **1**. Total ion chromatograms are shown for (a) esterification at the beginning (0 h) and the end (6 h) of the reaction, (b) the oxazolinone-cyclization reaction and (c) initial purification of **1** by semi-preparative HPLC after the *N*-methylation reaction. Final purification of **1** by further semi-preparative HPLC is shown in **Figure 2**. Compounds are indicated by a coloured box and numbered.  $[M+H]^+$  signals corresponding to each observed compound are indicated beside each coloured box.



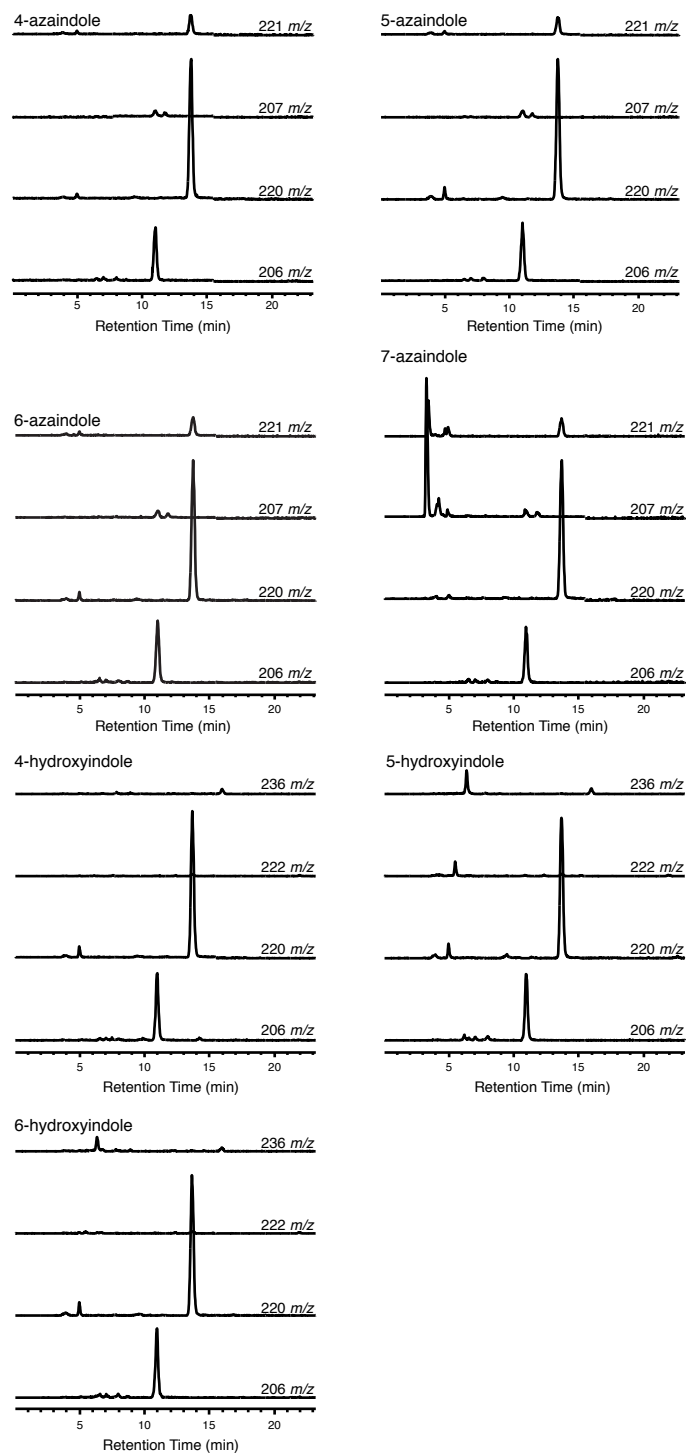
**Figure S4:** UV-vis traces obtained during LC-MS analysis of synthetic steps showing regeneration of **5**. Absorbance measurements were made at 280 nm. Traces show high levels of **5** regenerated after the oxazolinone-cyclization step in (a) and high levels of **5** remaining after *N*-methylation reaction in (b).



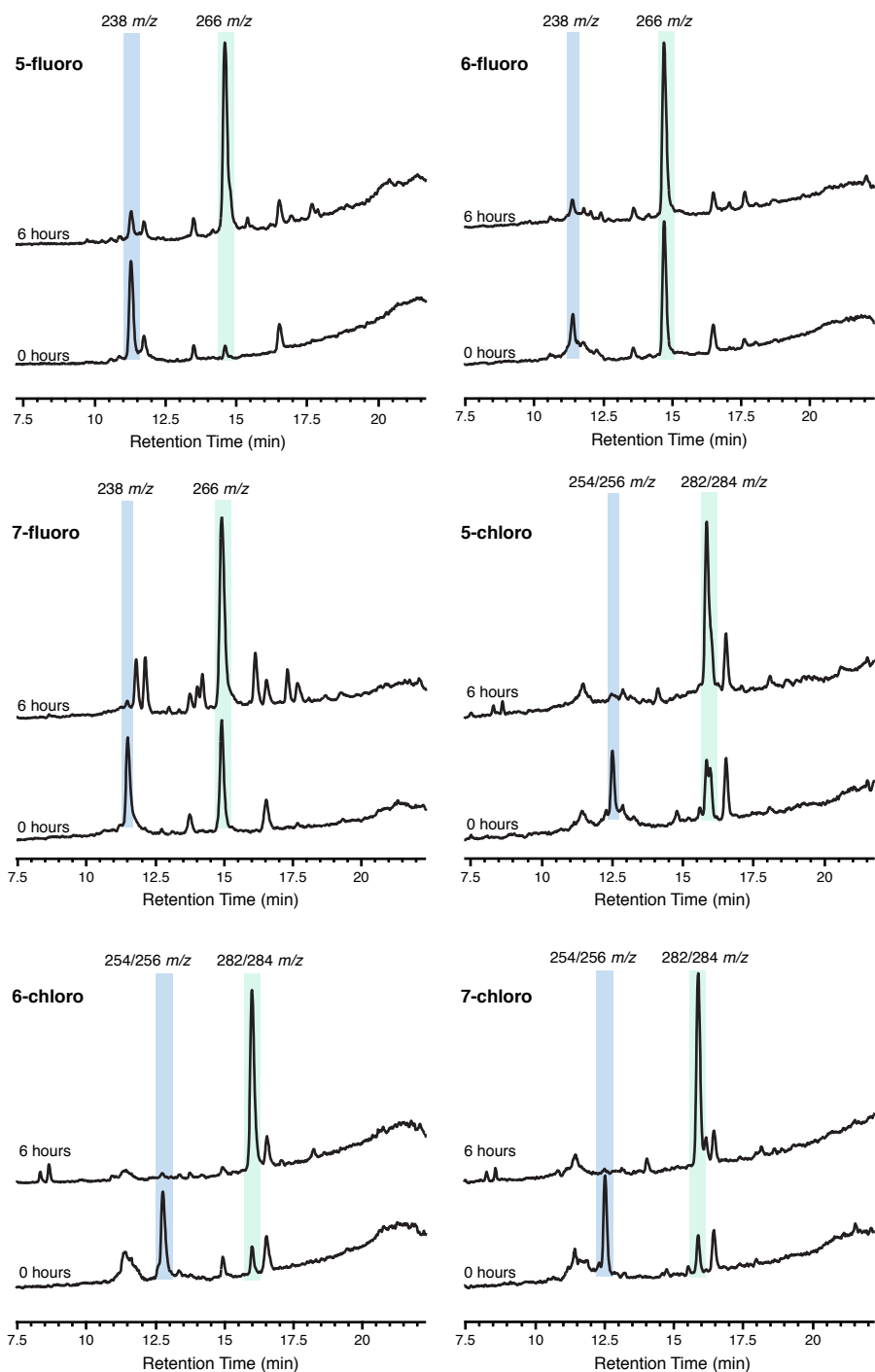
**Figure S5:** HPLC analysis of **5F-5** amounts under different feeding conditions. Amount of **5F-5** was approximated based on peak area measured at 280 nm. Amount of **5F-5** produced for 2.0 mM and 1.0 mM was only tested on the first day.



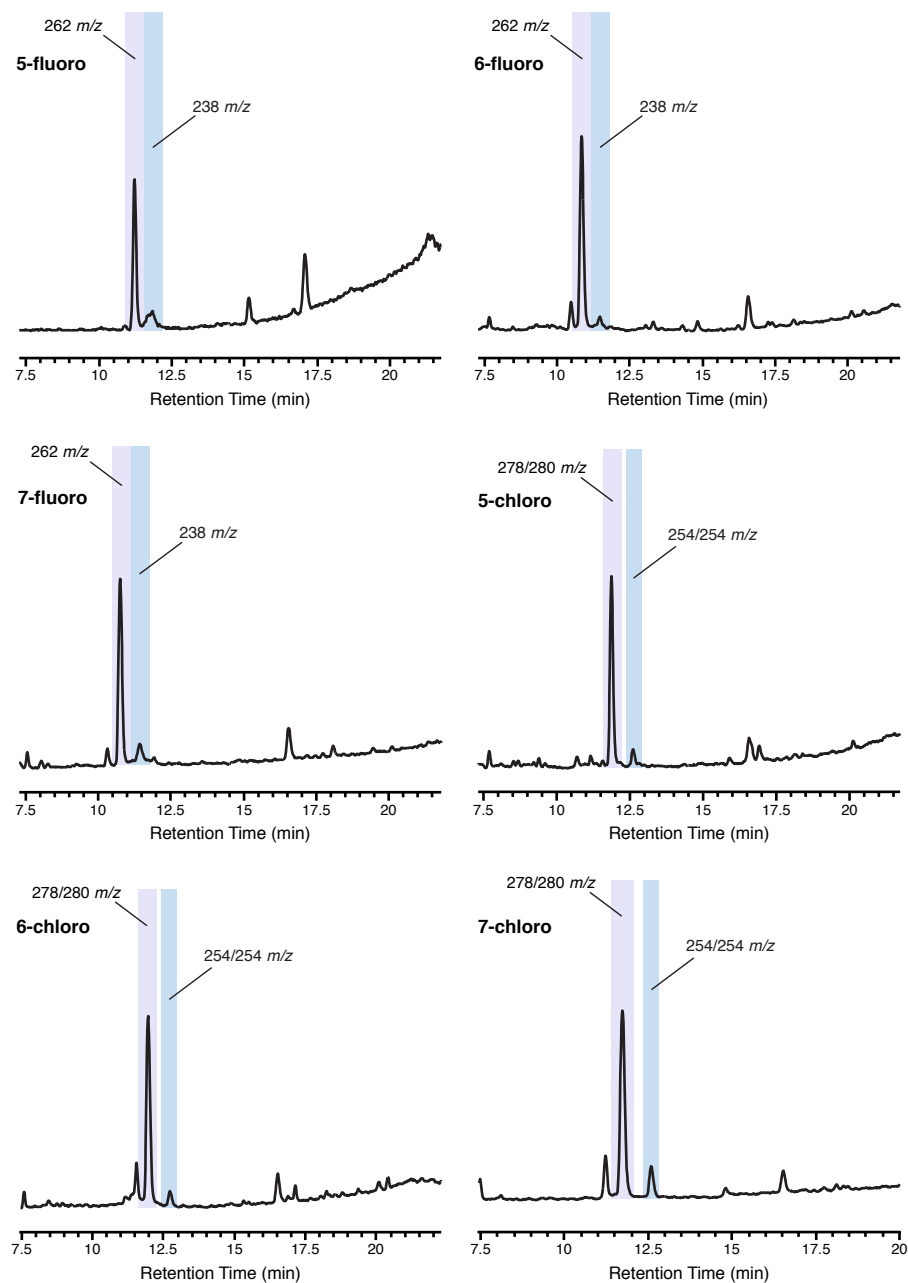
**Figure S6:** LC-MS analysis of halogen-substituted indole incorporation into **5** using *E. coli* I1234670TS. Each trace represents an extracted ion chromatogram of  $[M+H]^+$  masses for **6**, **5**, substituted **6** and substituted **5**.



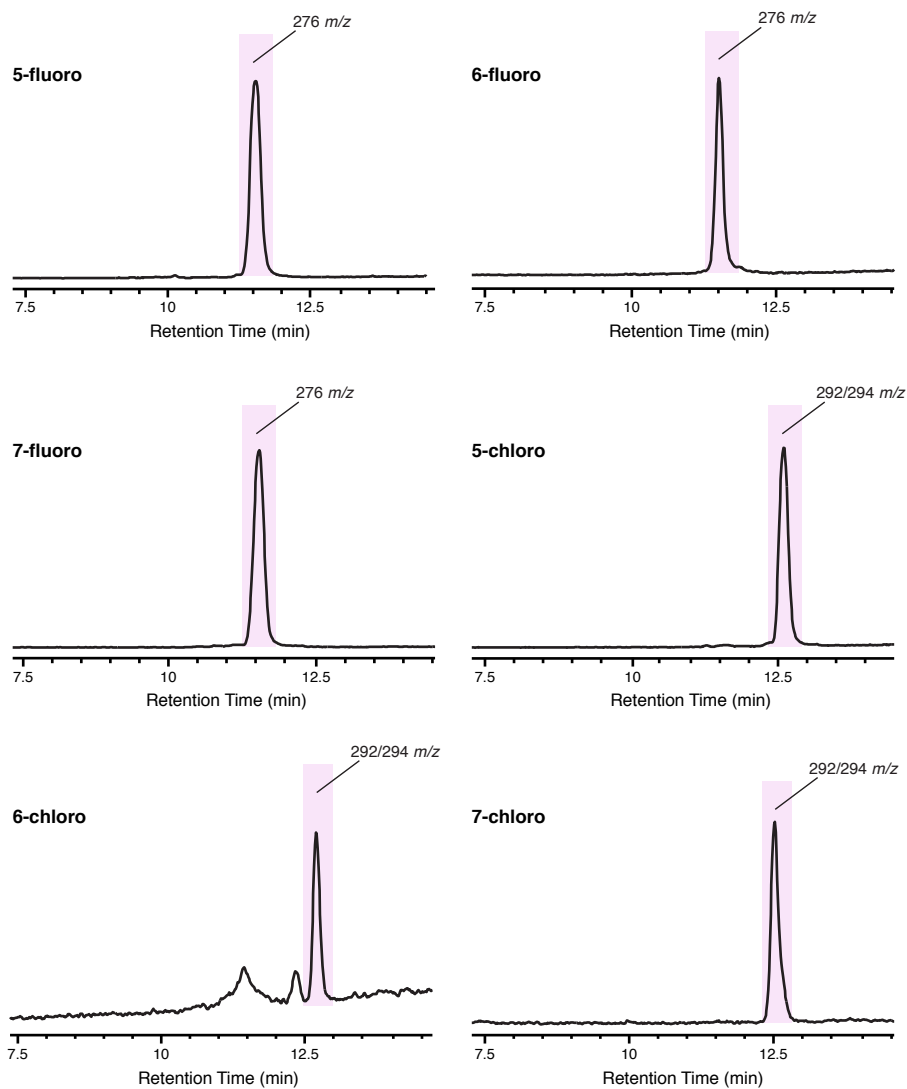
**Figure S7:** LC-MS analysis of hydroxyindole or azaindole incorporation into **5** using *E. coli* I1234670TS. Each trace represents an extracted ion chromatogram of  $[M+H]^+$  masses for **6**, **5**, derivatives of **6** and derivatives of **5**. 7-azaindole, 5-hydroxyindole and 6-hydroxyindole show some evidence of incorporation.



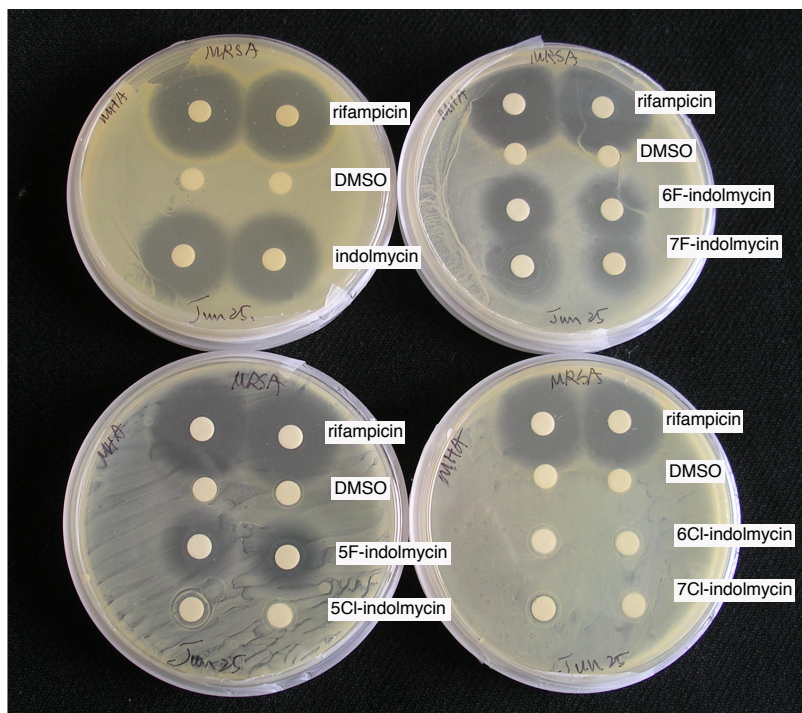
**Figure S8:** LC-MS analysis of 5-derivative esterification. Total ion chromatograms are shown for each derivative (5-fluoro, 6-fluoro, 7-fluoro, 5-chloro, 6-chloro and 7-chloro) at the beginning of the reaction, immediately after mixing reagents (0 h) and the end of the reaction (6 h). The starting materials, 5-derivatives, and the products, 7-derivatives, are indicated by a blue or green box, respectively. The ion masses for each compound are given above the corresponding boxes.



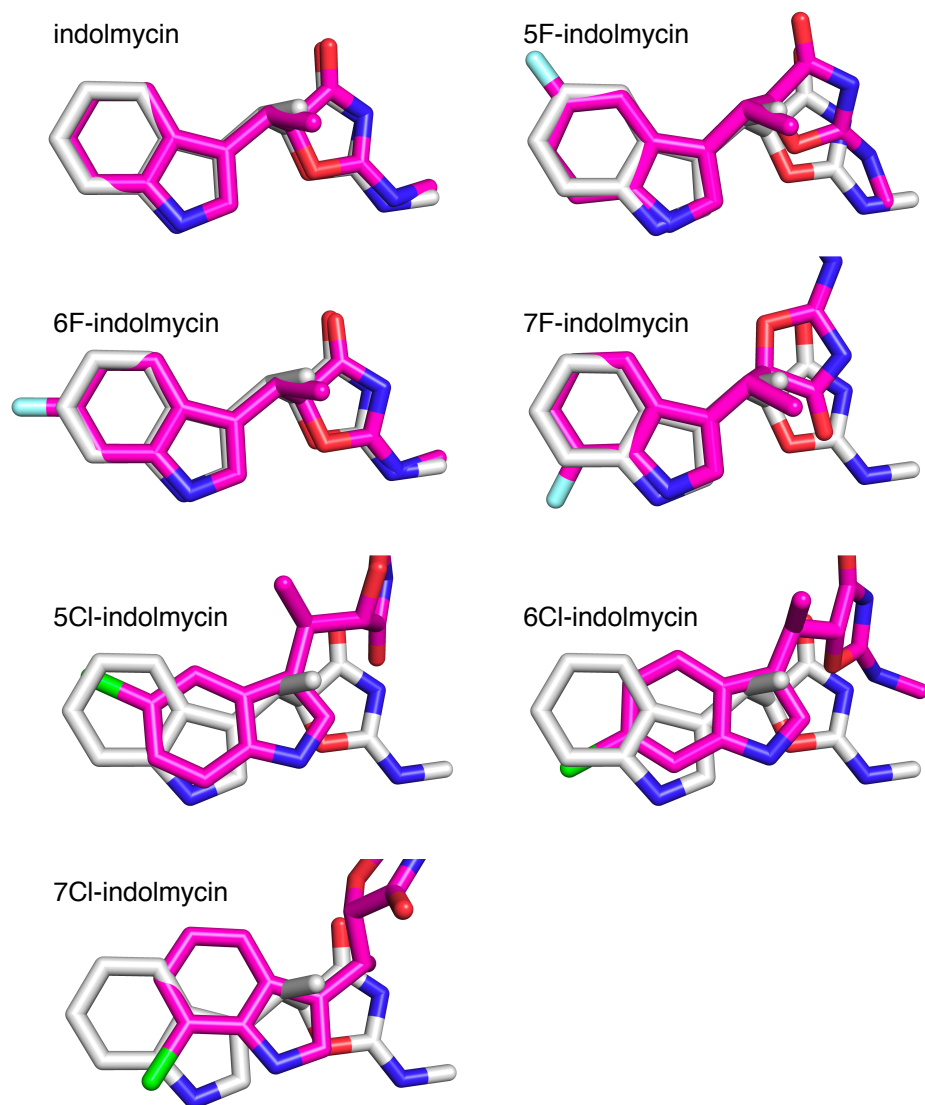
**Figure S9:** LC-MS analysis of 7-derivative oxazolinone-cyclizations. Total ion chromatograms are shown for each derivative (5-fluoro, 6-fluoro, 7-fluoro, 5-chloro, 6-chloro and 7-chloro). Oxazolinone-cyclized products, **8**-derivatives, are indicated with a purple box and **5**-derivative side-products generated during the reaction are shown with a blue box. Ion masses for each compound are indicated.



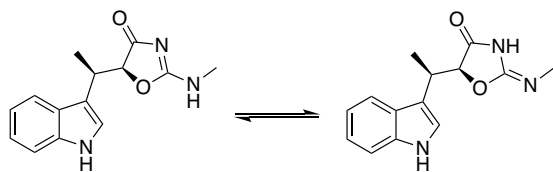
**Figure S10:** LC-MS analysis of **8**-derivative *N*-methylation. Total ion chromatograms are shown for each derivative (5-fluoro, 6-fluoro, 7-fluoro, 5-chloro, 6-chloro and 7-chloro) after semi-preparative HPLC purification. **1**-derivative products are indicated with a pink box. Ion masses for each product are indicated.



**Figure S11:** Disk diffusion assay of **1** and its derivatives against MRSA. Rifampicin (1  $\mu\text{g}$ ) and DMSO (0.5%) were used as positive and negative controls, respectively. 10  $\mu\text{g}$  of **1**, 20  $\mu\text{g}$  of **6F-1** and **7F-1** and 30  $\mu\text{g}$  of **5F-1**, **5Cl-1**, **6Cl-1** and **7Cl-1** were loaded onto each disk. Compound **1** showed the highest activity with a zone of inhibition visible when 10  $\mu\text{g}$  of the compound was loaded onto each disk. **6F-1** and **7F-1** showed a zone of inhibition at 20  $\mu\text{g}$  per disk while **5F-1** showed inhibition at 30  $\mu\text{g}$  per disk.



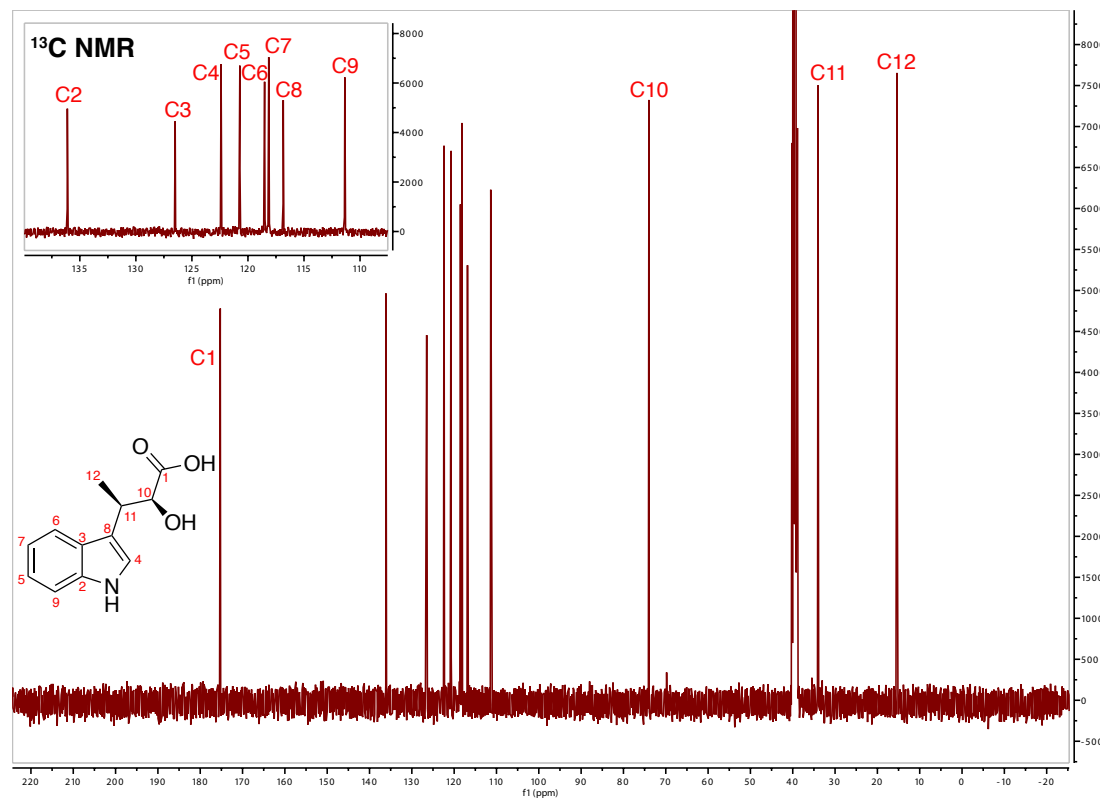
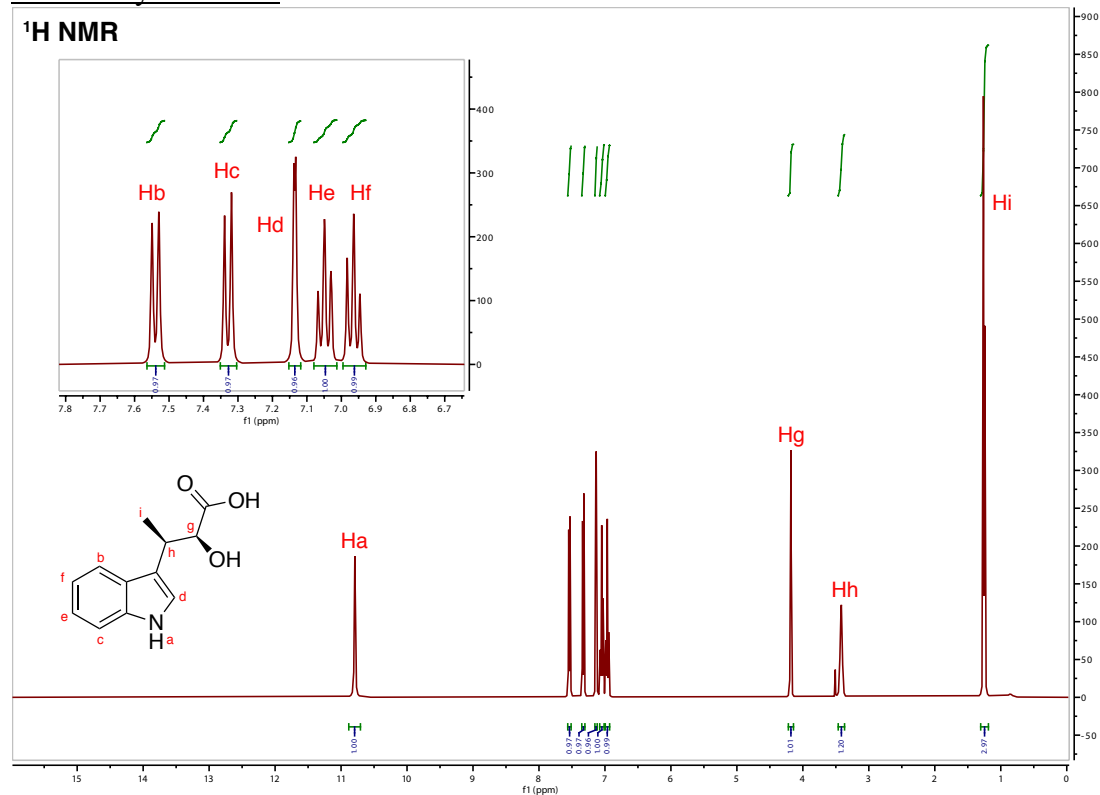
**Figure S12:** Docking of indolmycin derivatives made in this study into an indolmycin-bound crystal structure of TrpRS from *Bacillus stearothermophilus* (PDB: 5DK4). Docked molecules (magenta) are compared with active site-bound indolmycin (white) from the crystal structure. Binding modes for the indole rings of chlorinated analogs could not be matched with the crystal structure. Oxazolinone conformations for fluorinated compounds may have differed from the crystal structure because other ligands in the active site which interact with the oxazolinone ring, including ATP and  $Mg^{2+}$ , were not included in the docking model.

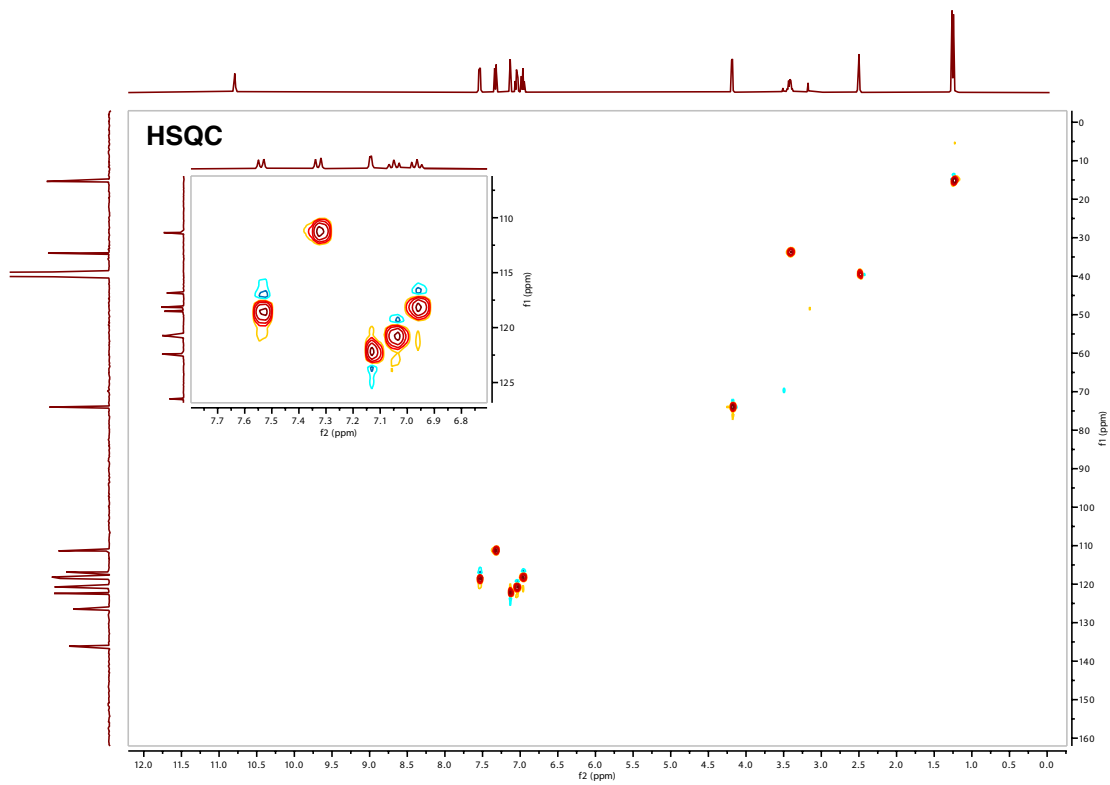
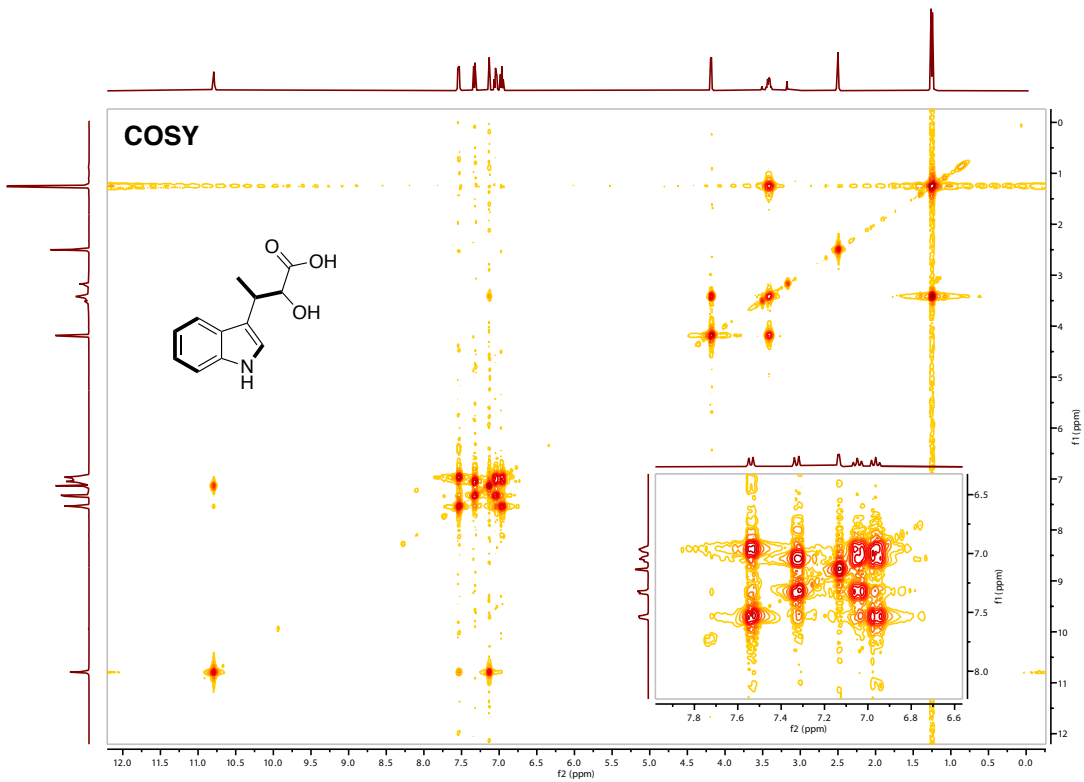


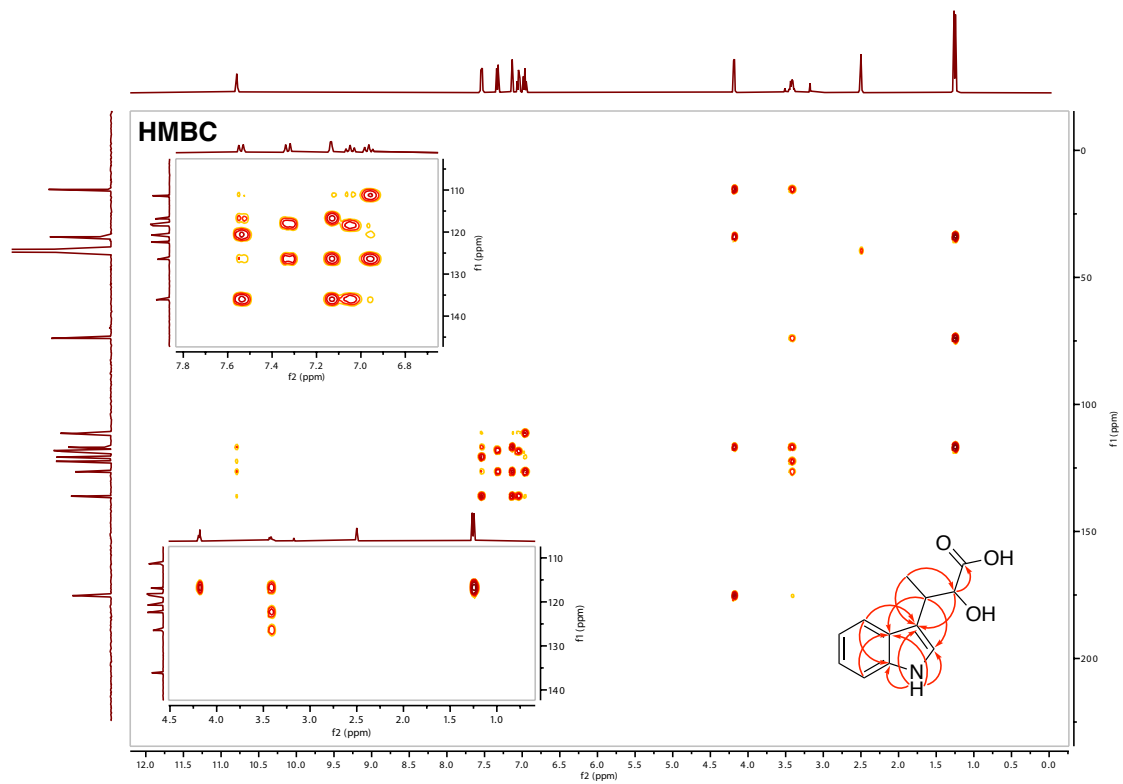
**Figure S13:** Predicted tautomeric isomers of indolmycin observed from  $^1\text{H}$  NMR spectra with the natural tautomer on the left.

# NMR Spectra

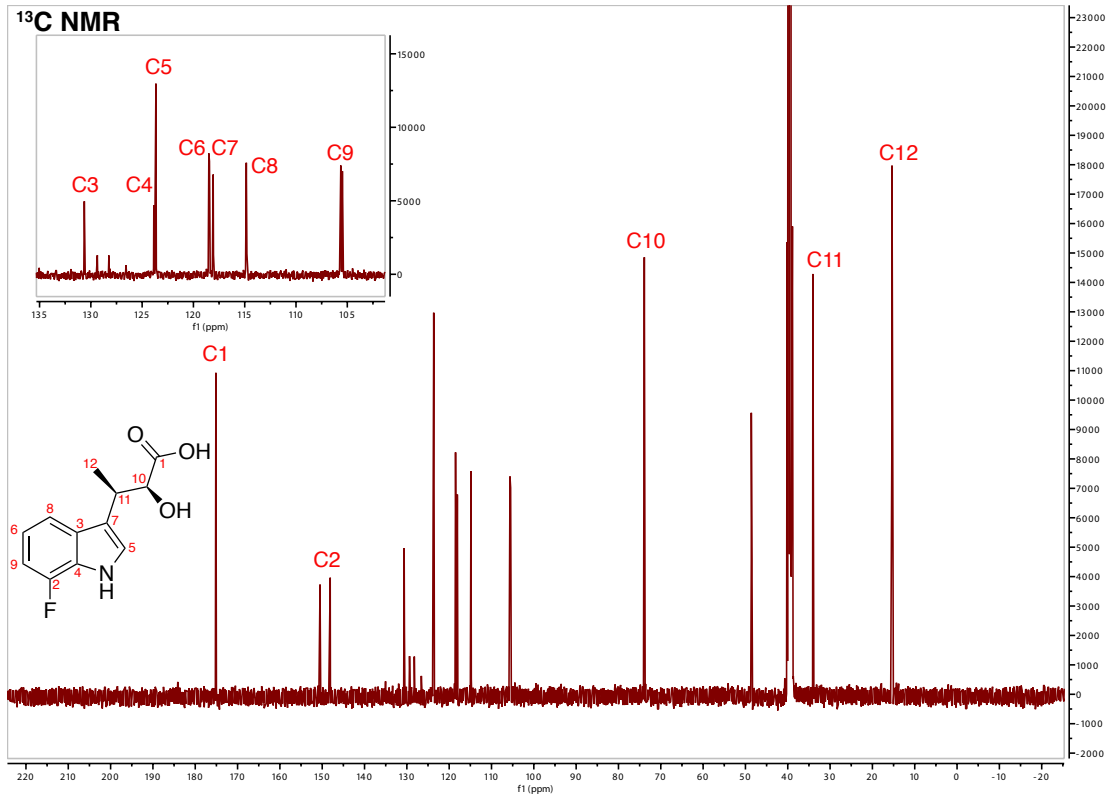
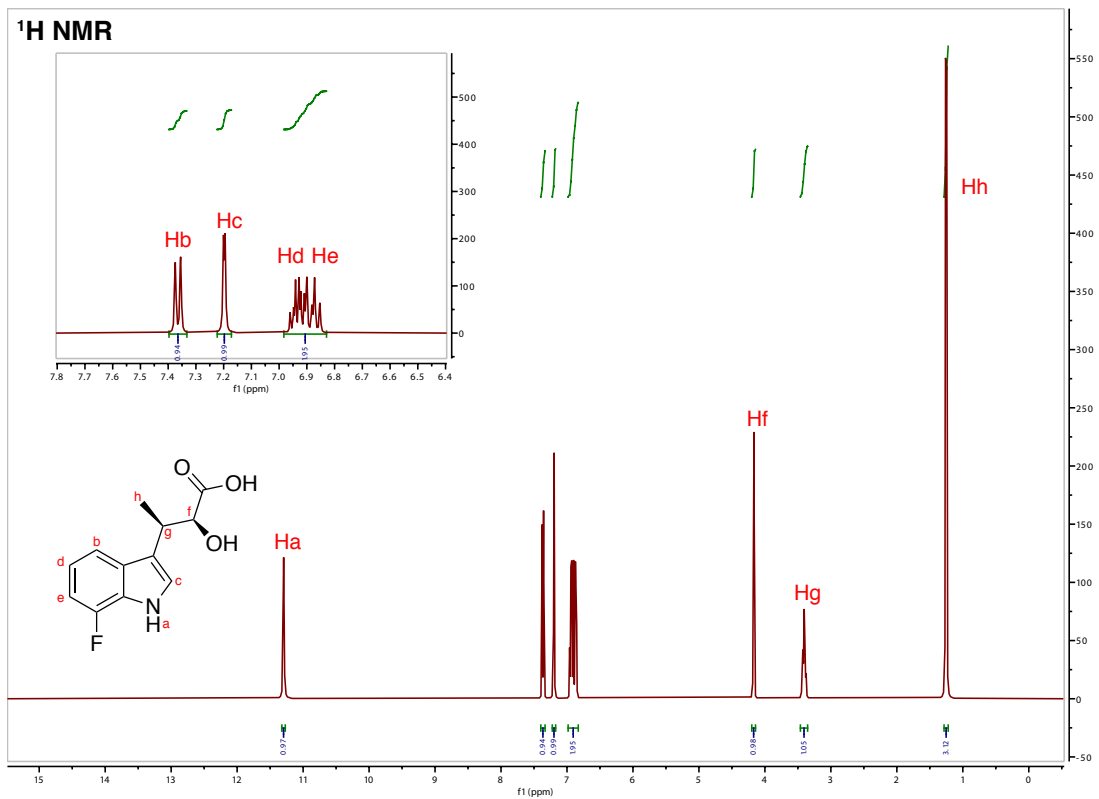
## 5: indolmycenic acid

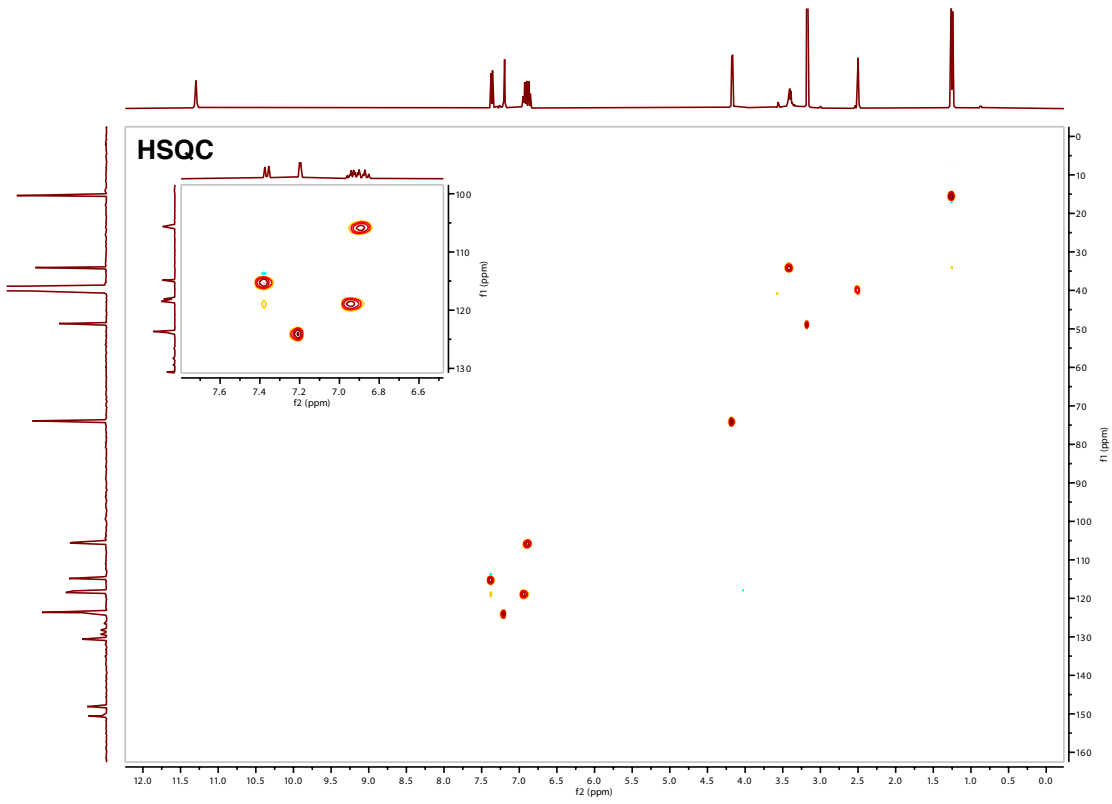
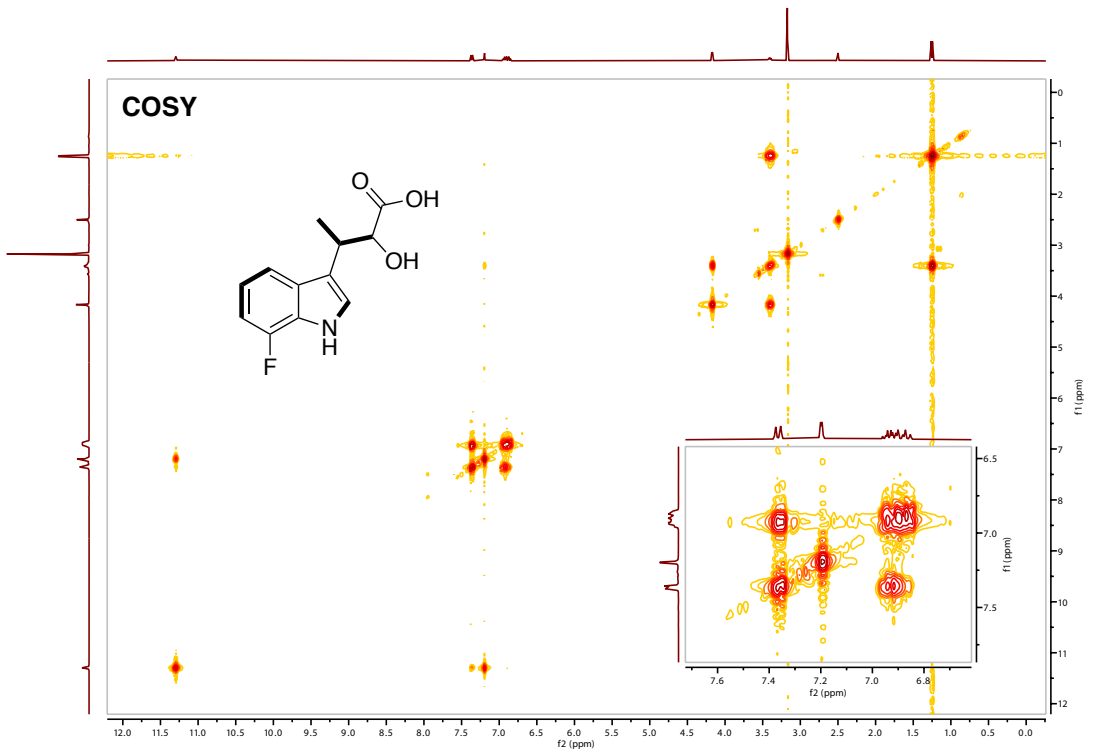


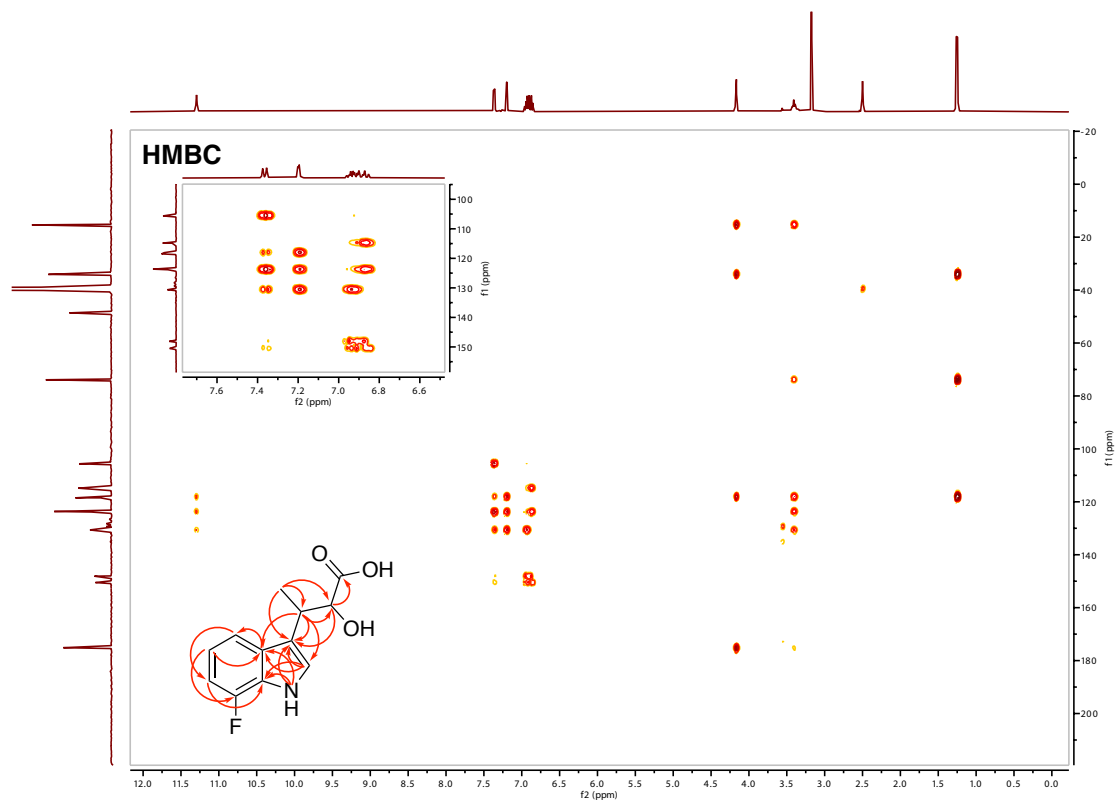




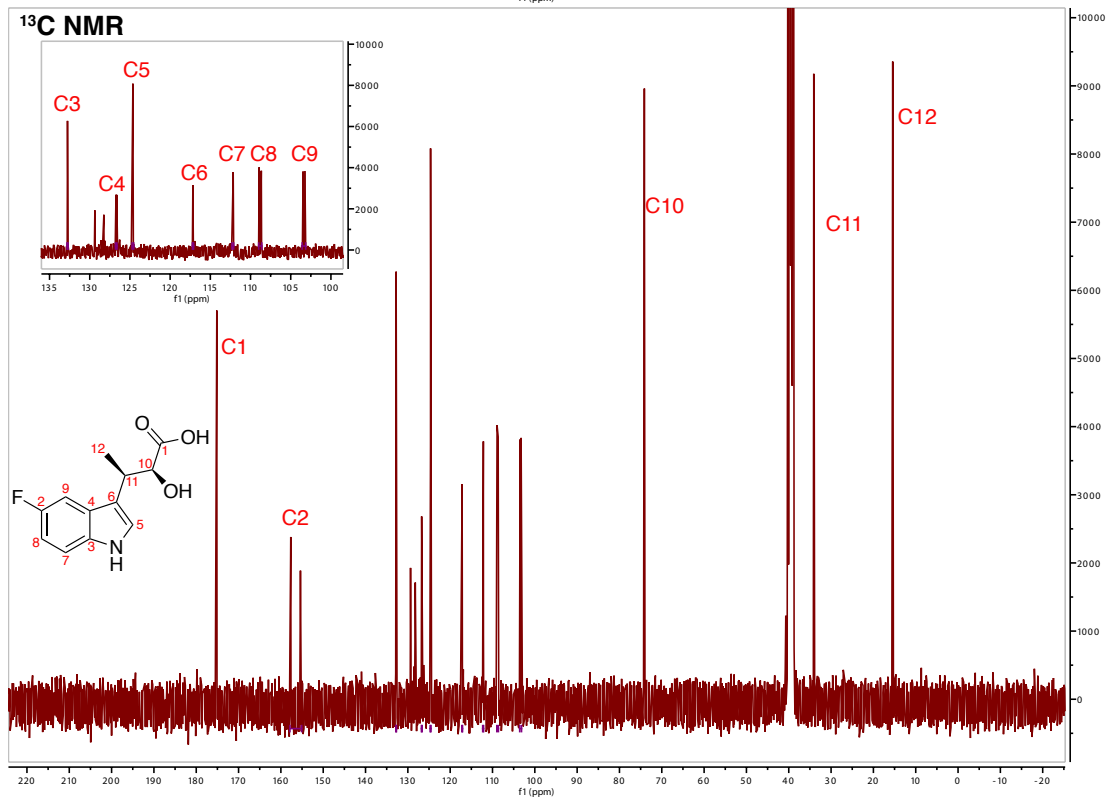
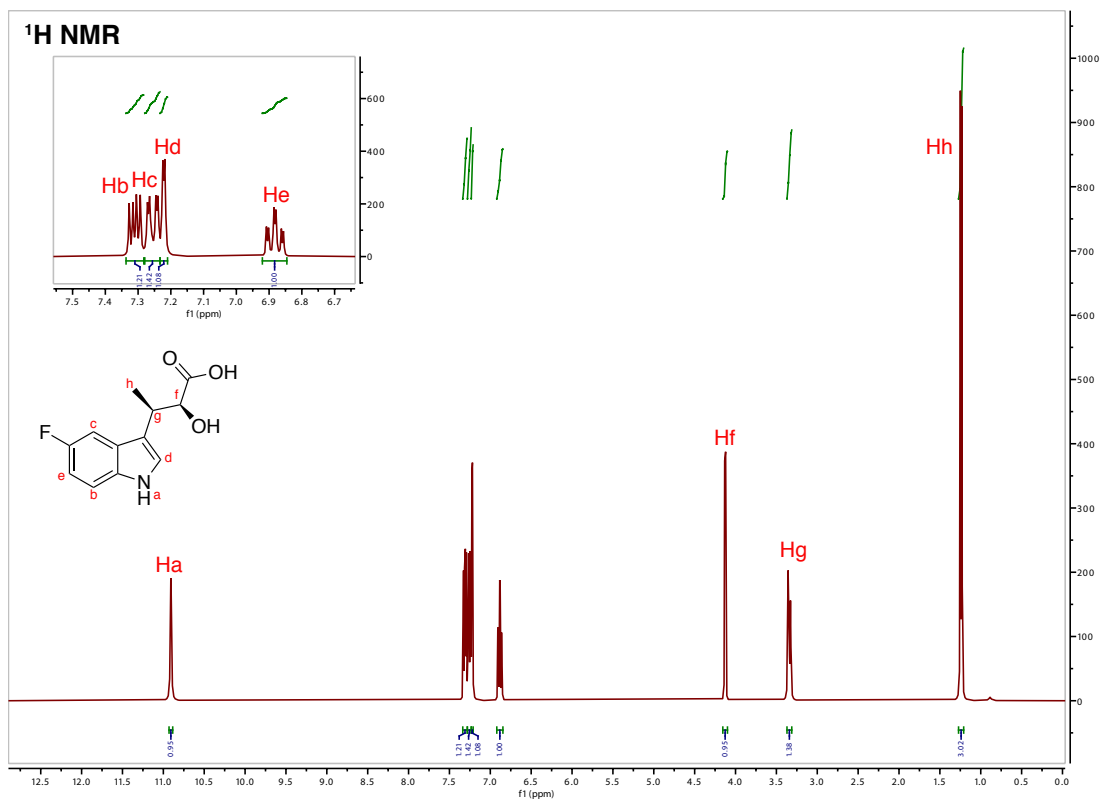
# 7F-5: 7-fluoro-indolmycenic acid



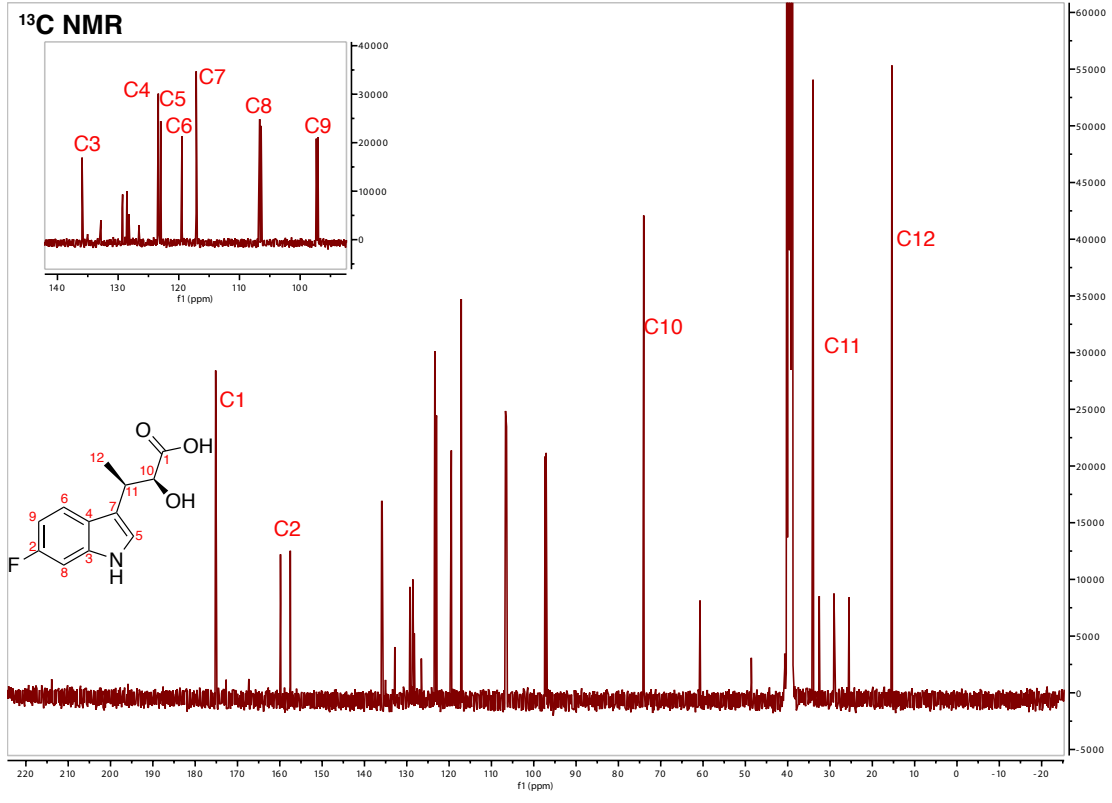
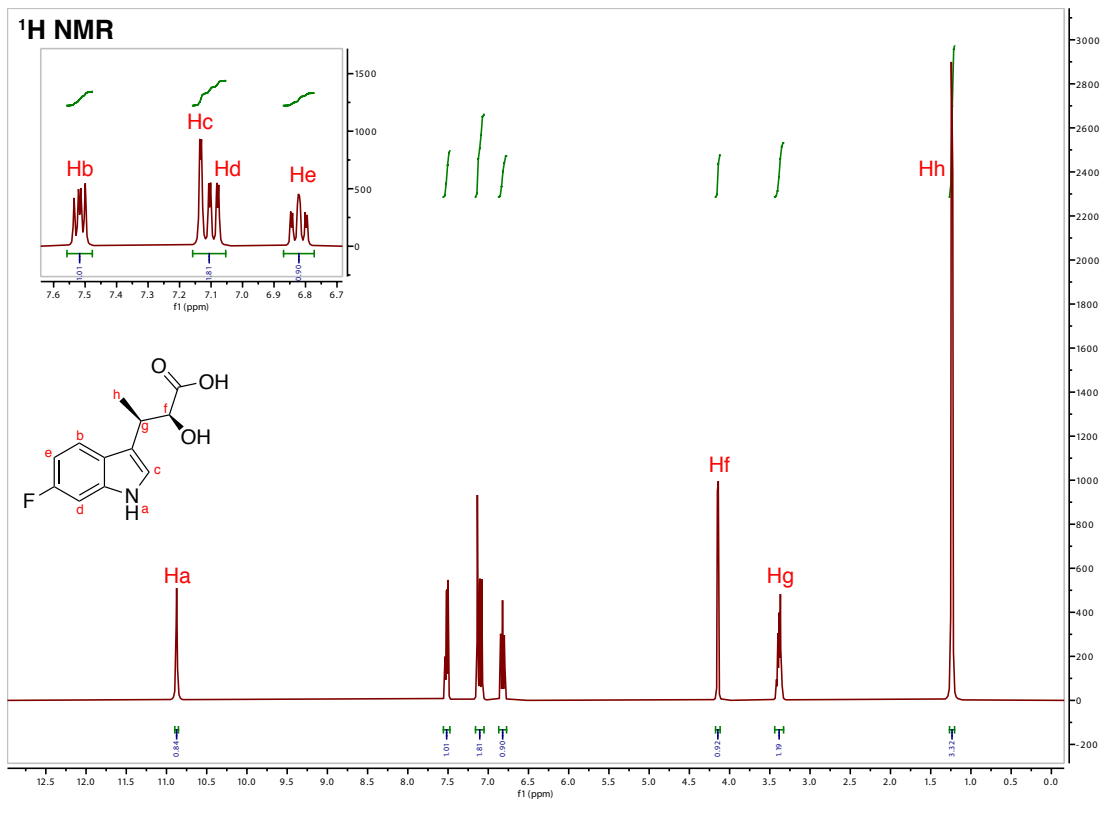




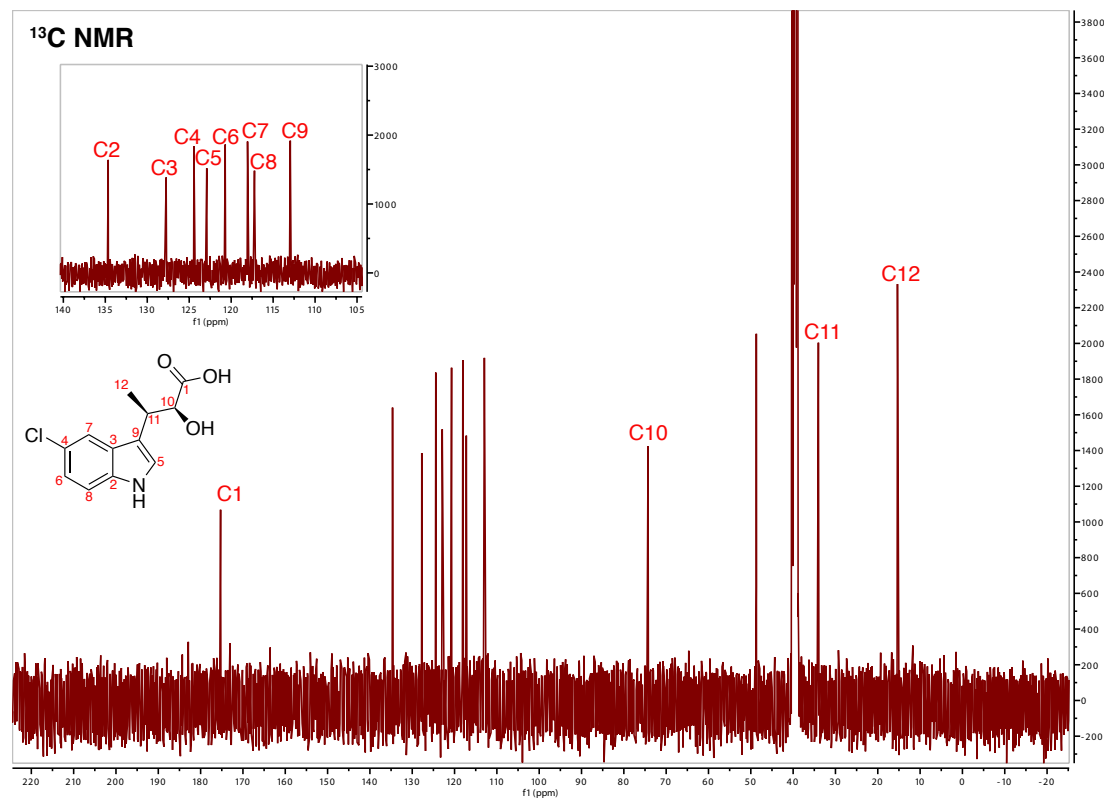
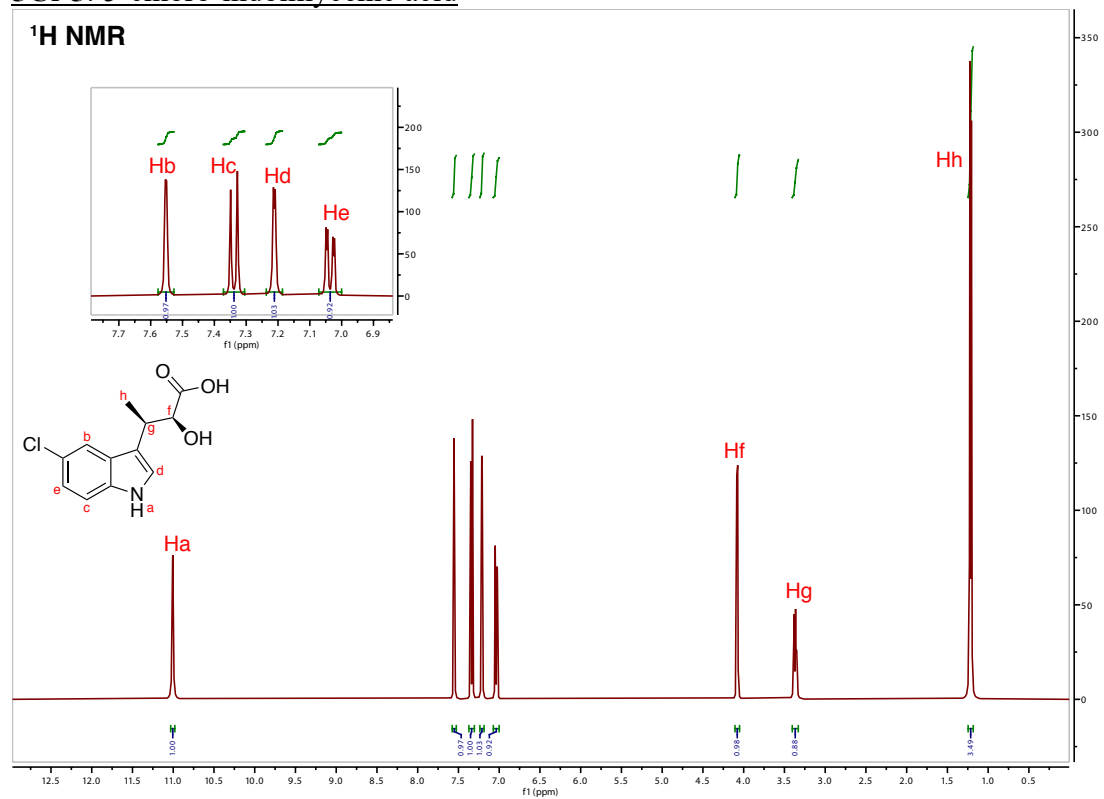
### 5F-5: 5-fluoro-indolmycenic acid



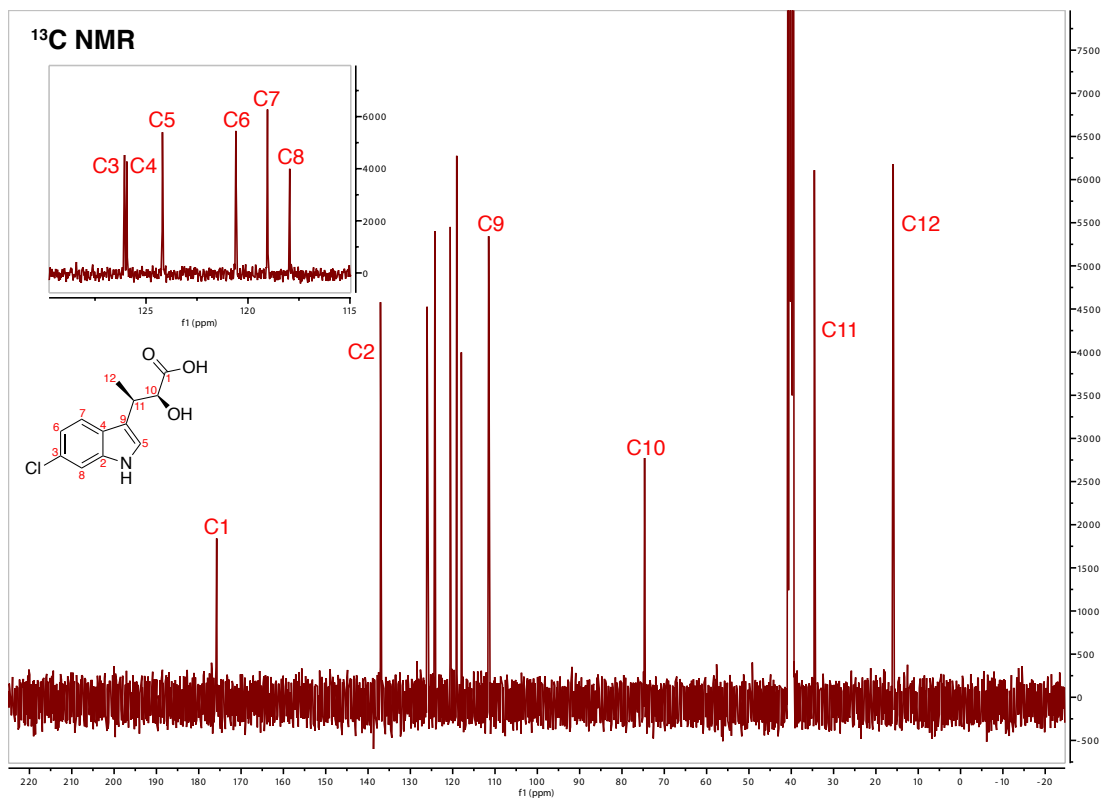
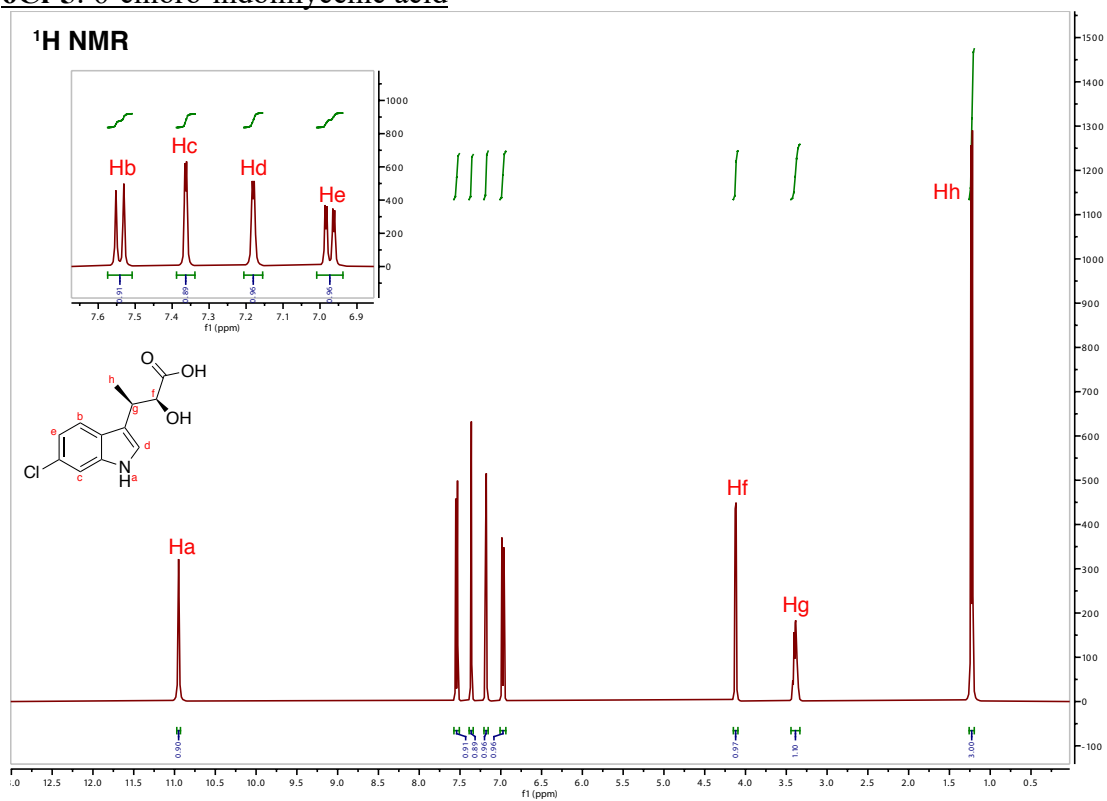
# 6F-5: 6-fluoro-indolmycenic acid



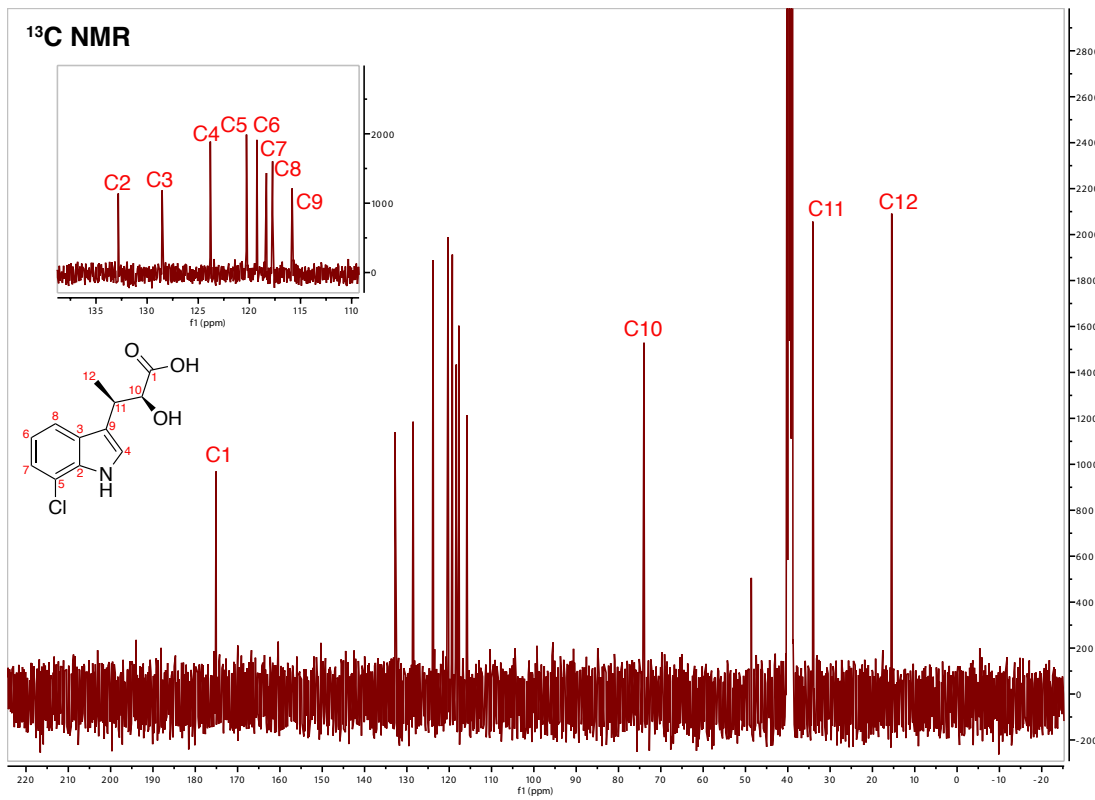
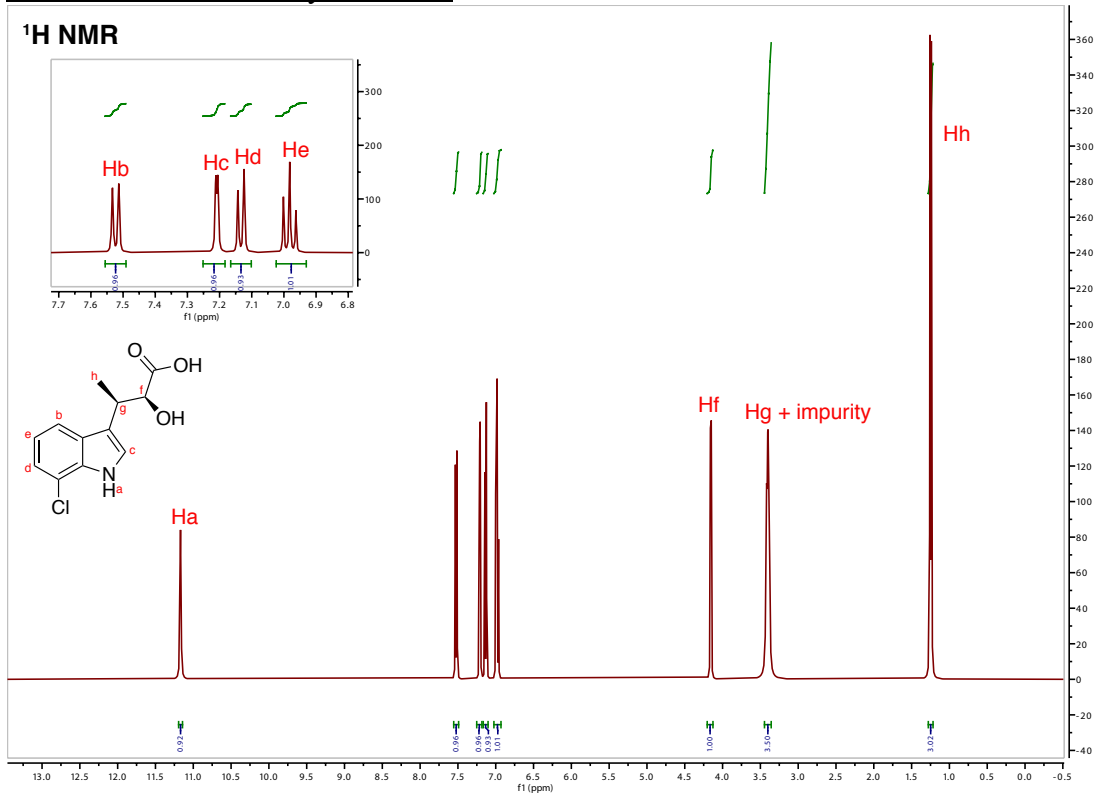
# 5Cl-5: 5-chloro-indolmycenic acid



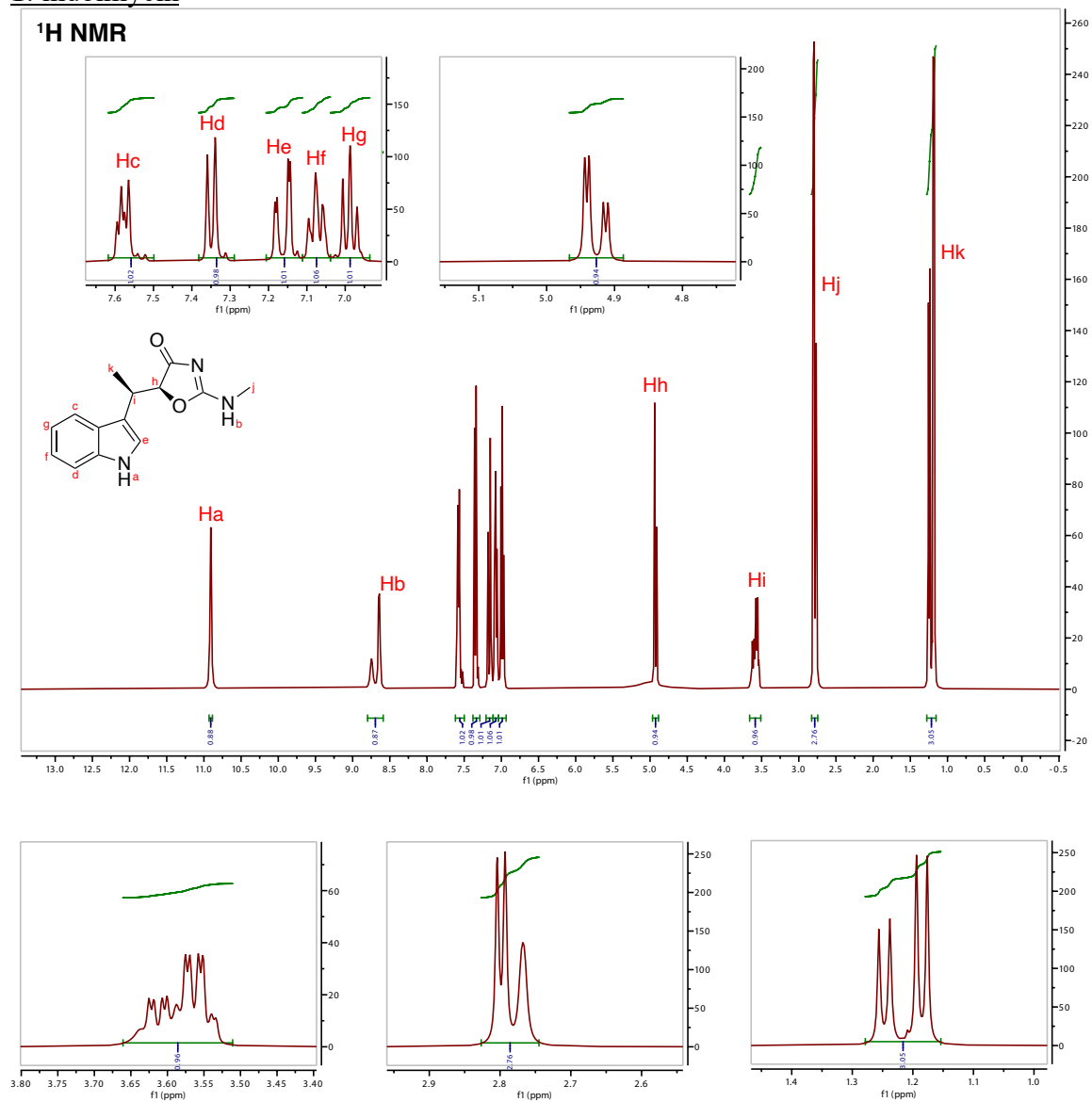
# 6Cl-5: 6-chloro-indolmycenic acid

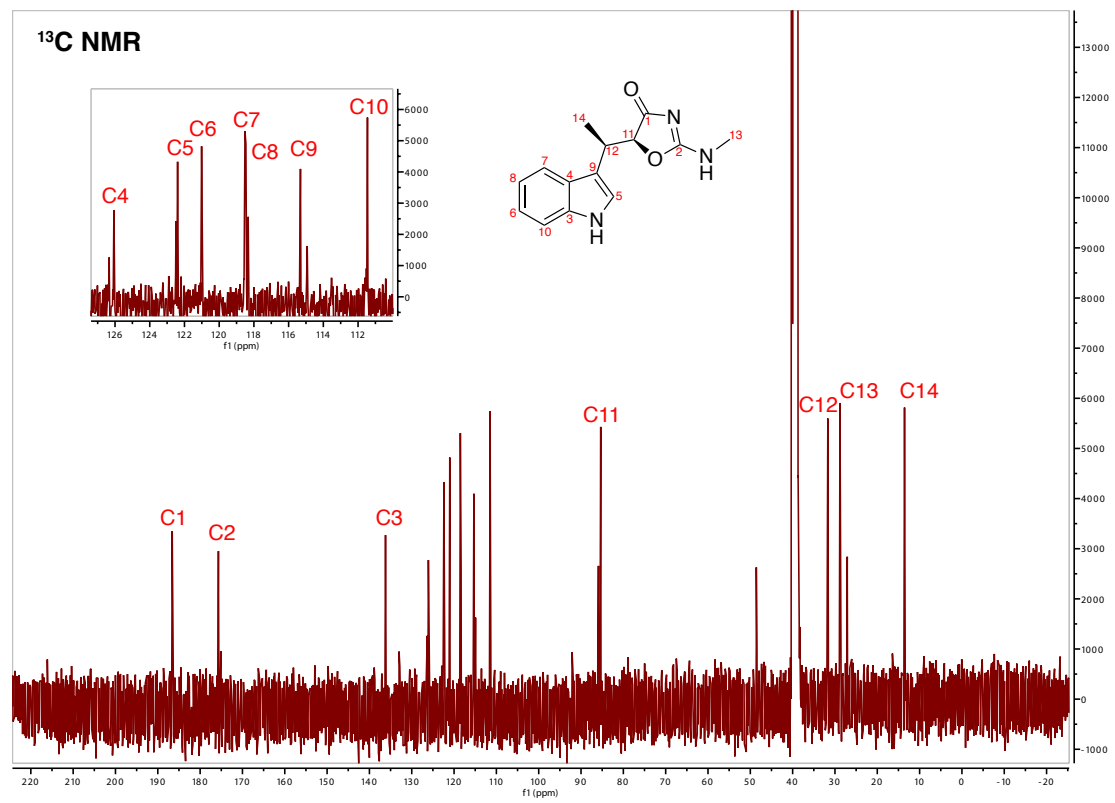


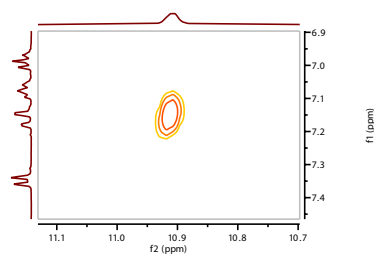
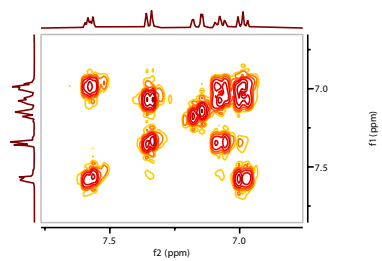
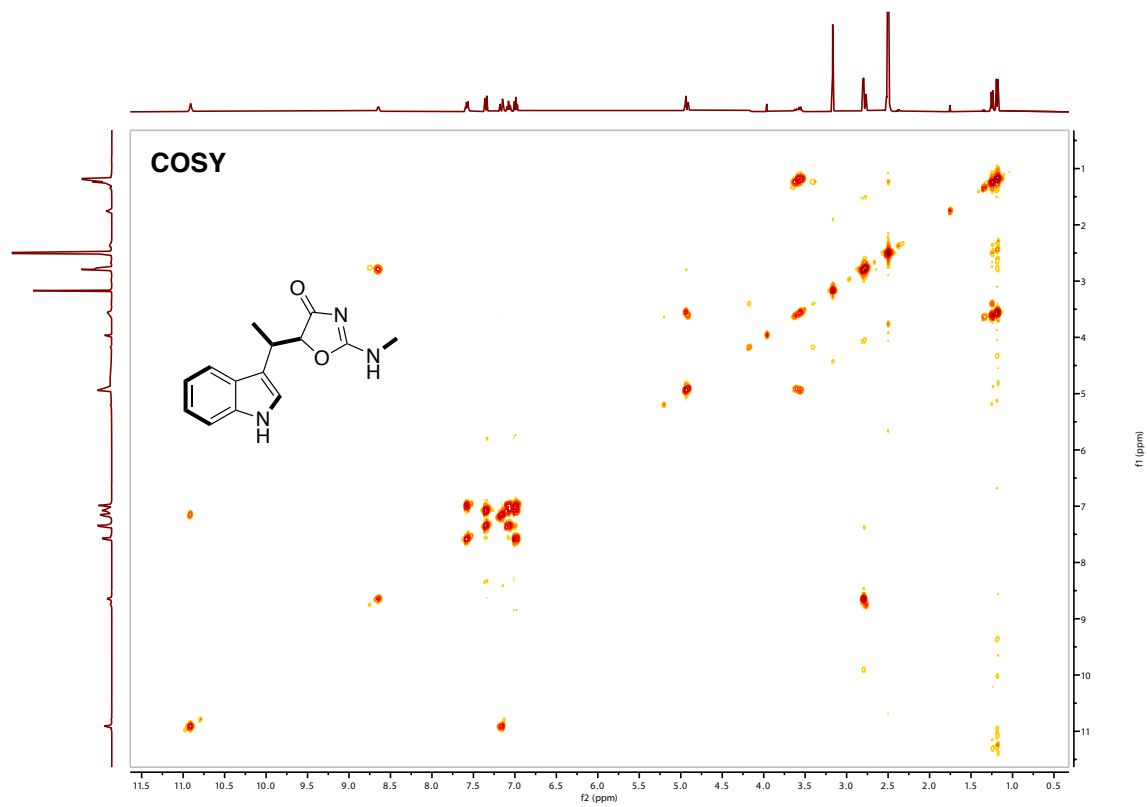
# 7Cl-5: 7-chloro-indolmycenic acid

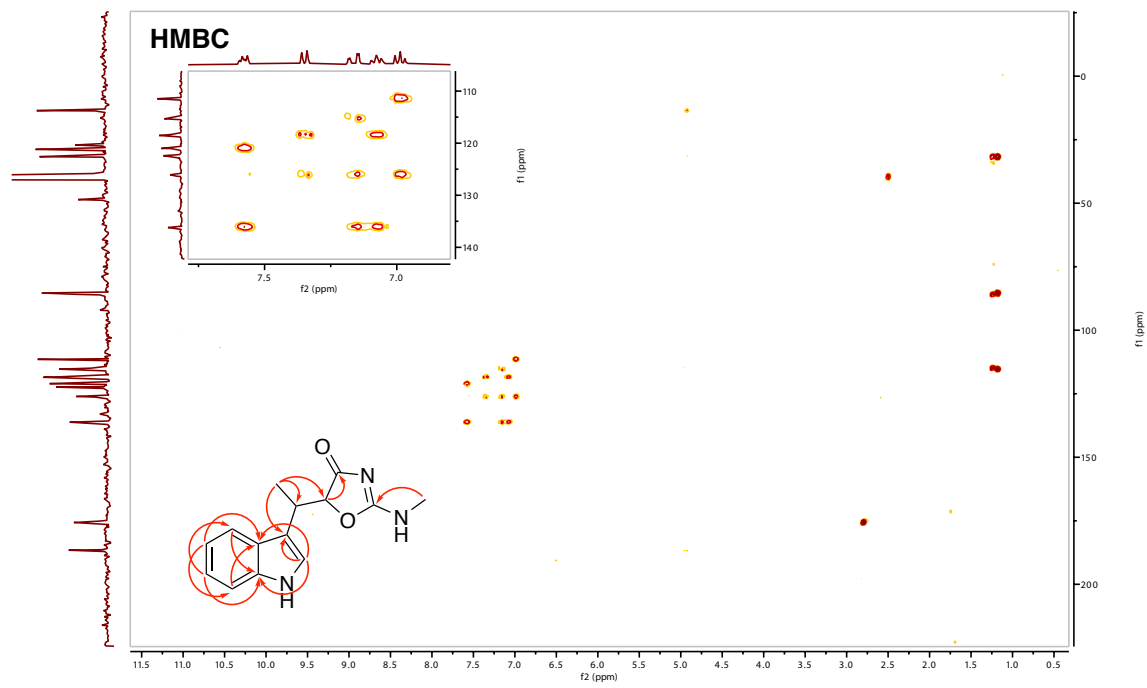
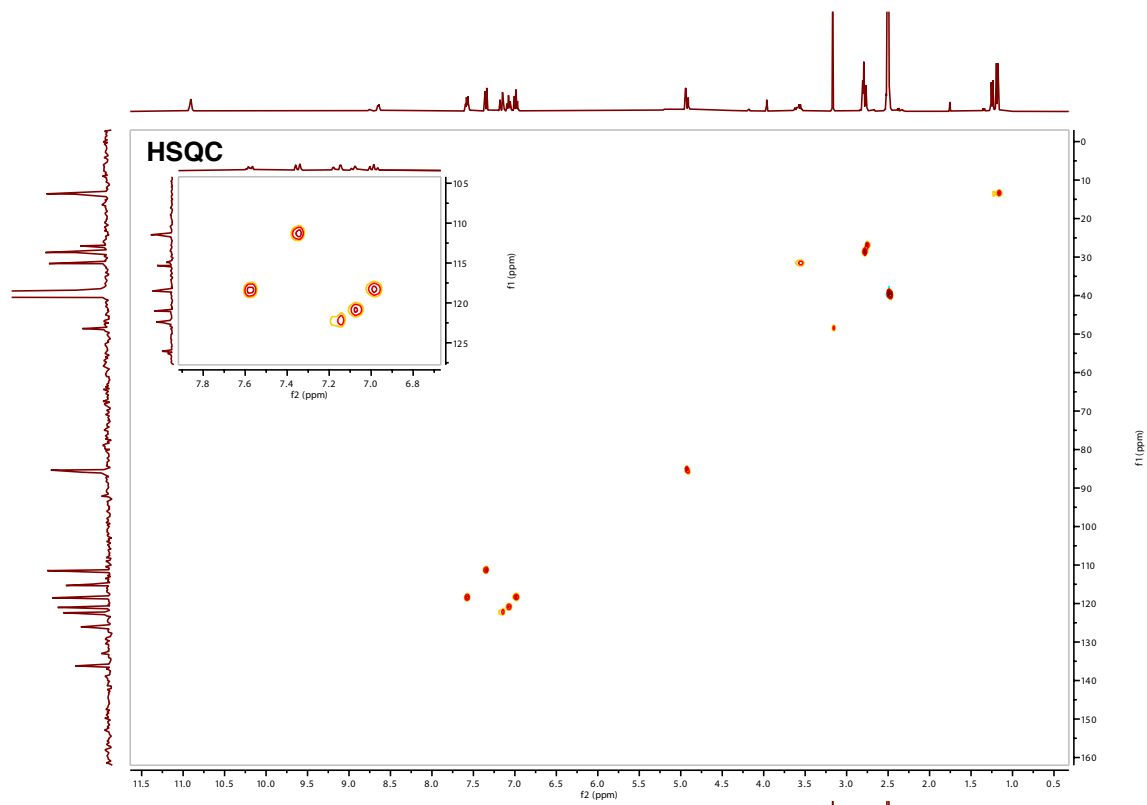


# 1: indolmycin

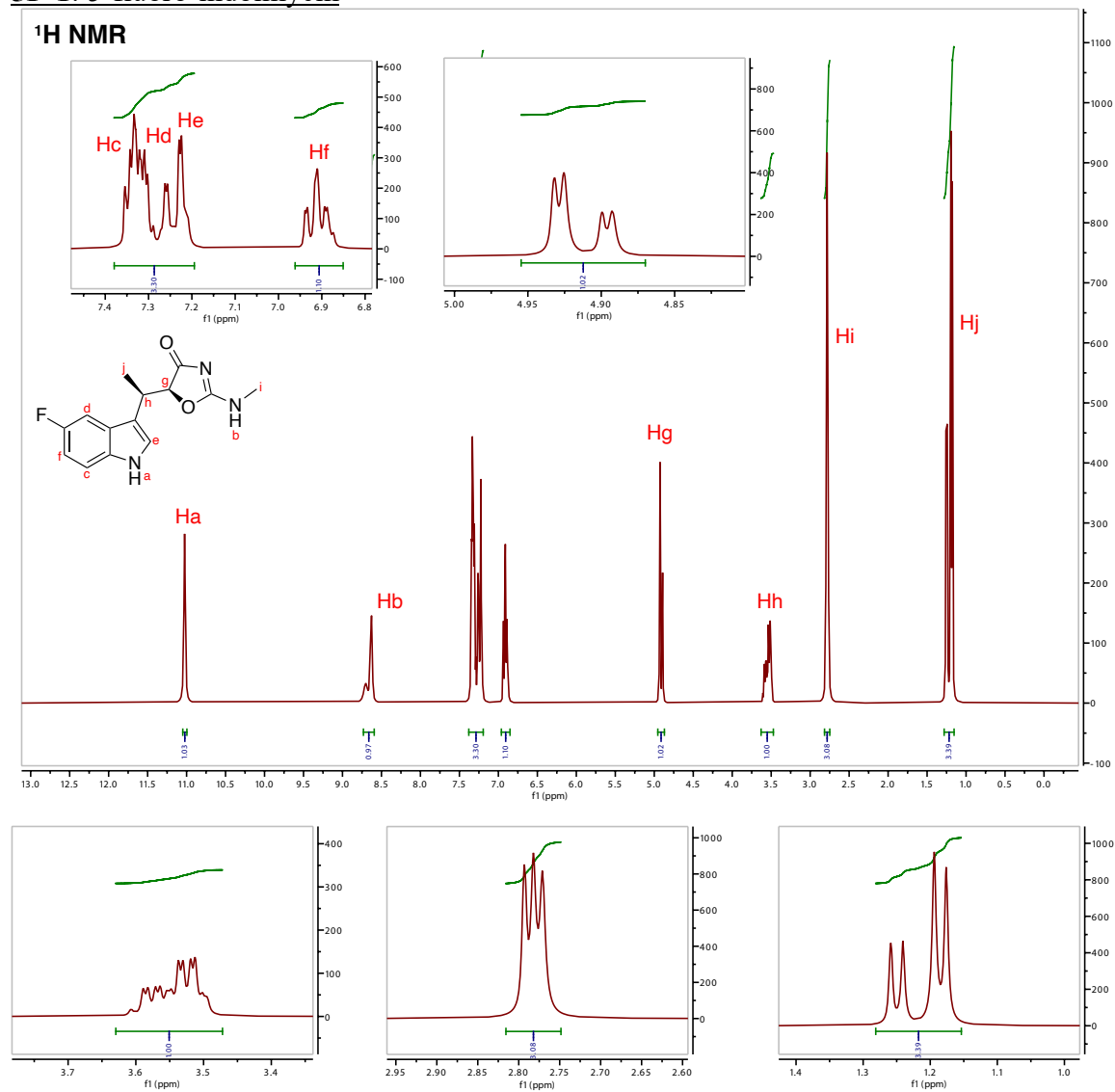


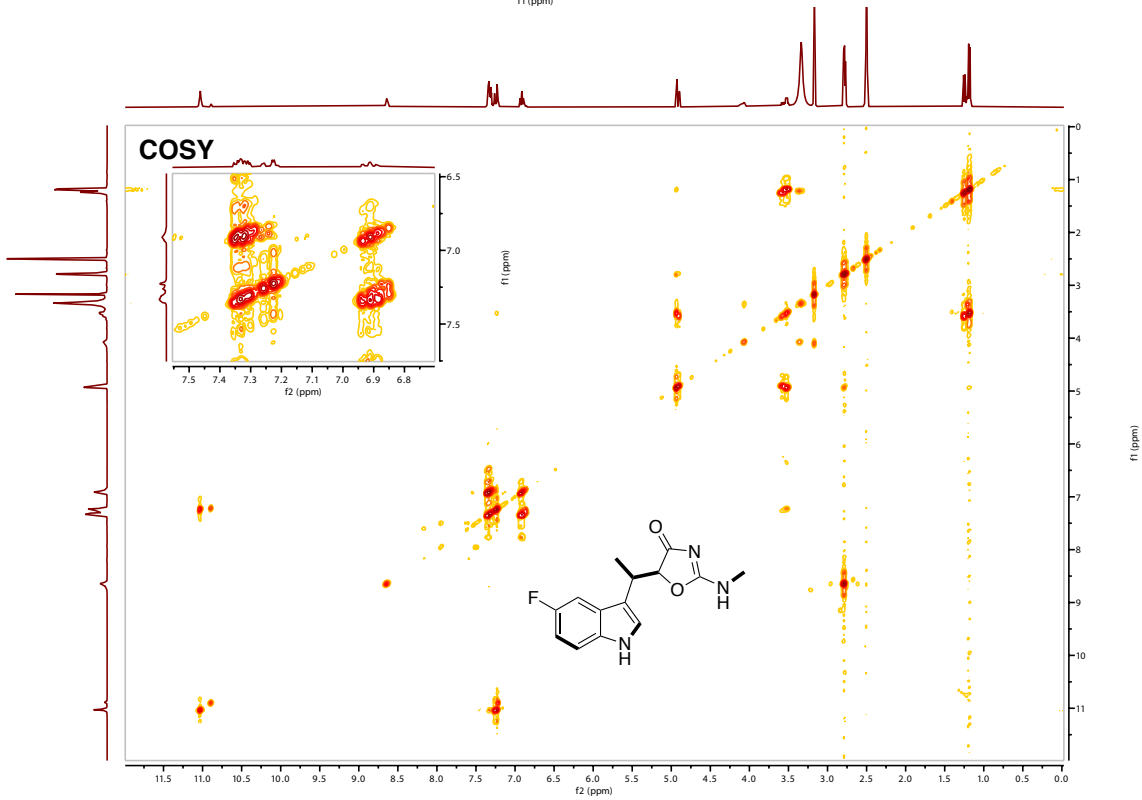
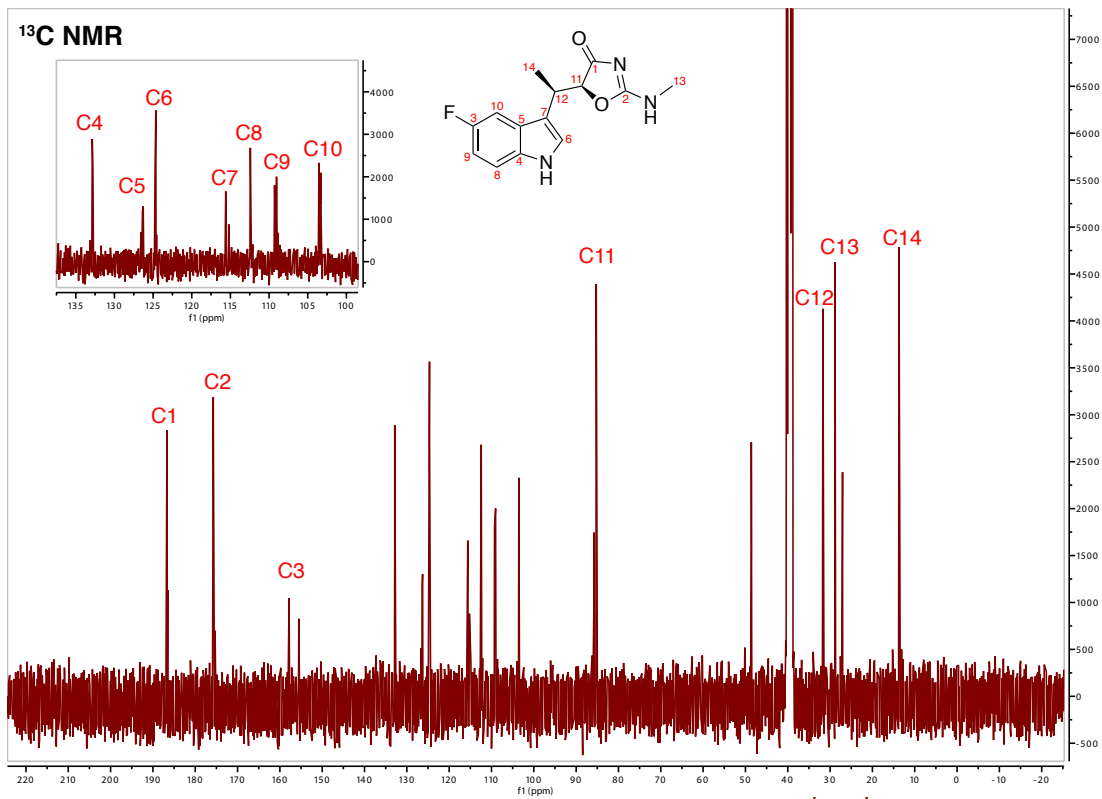


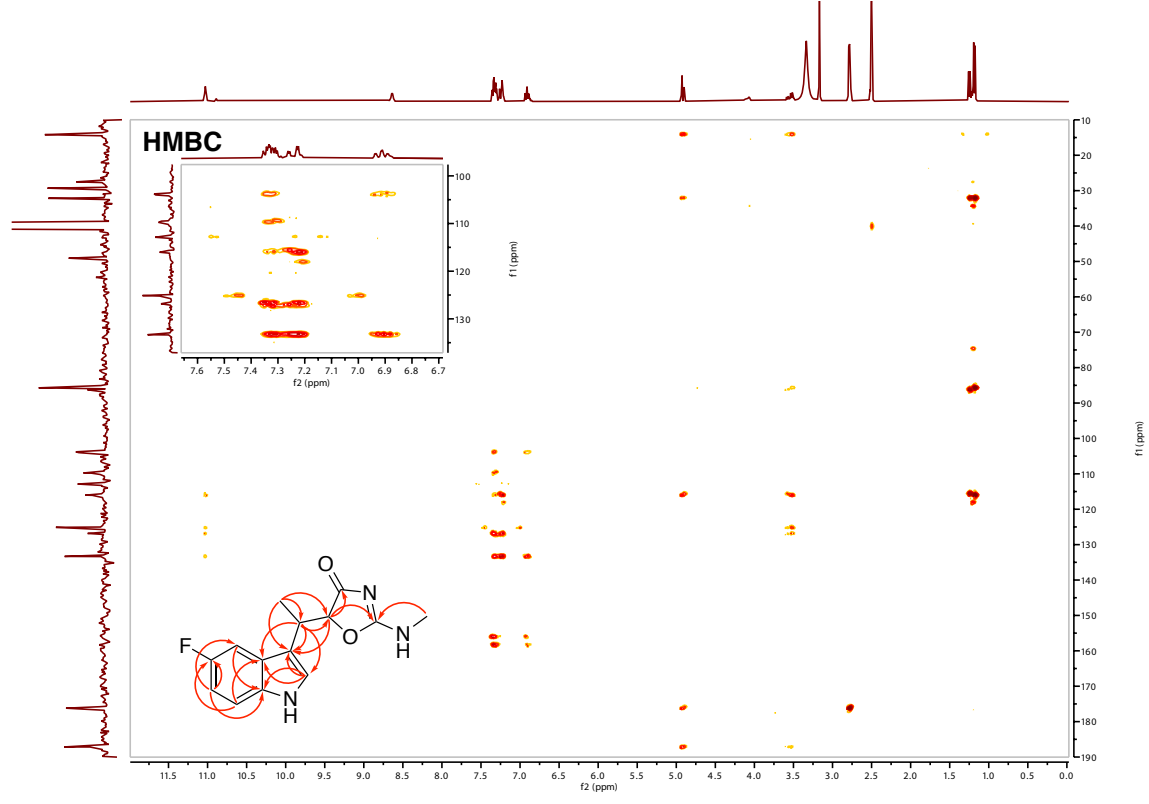
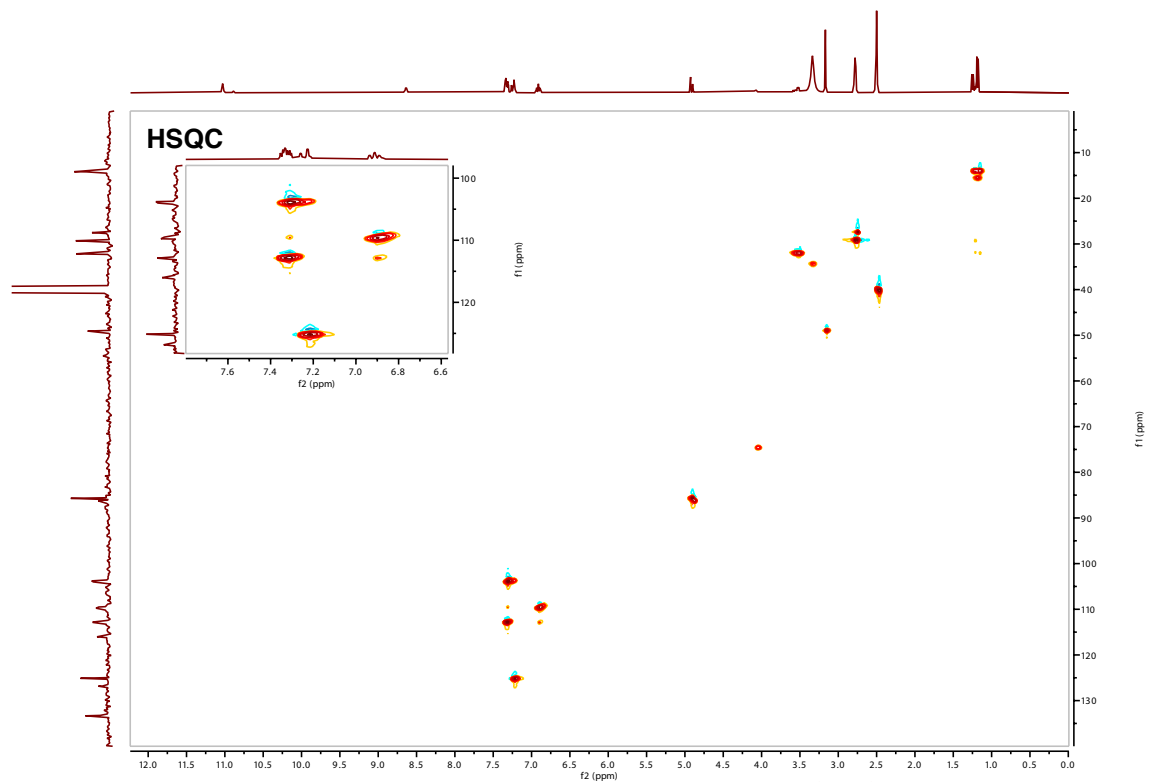


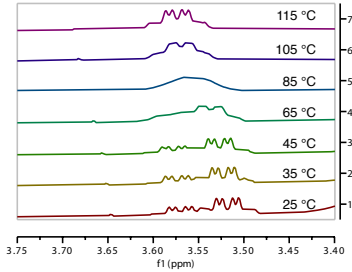
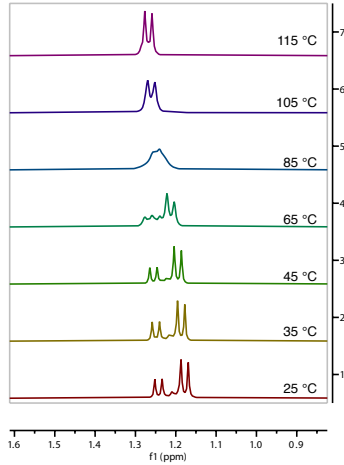
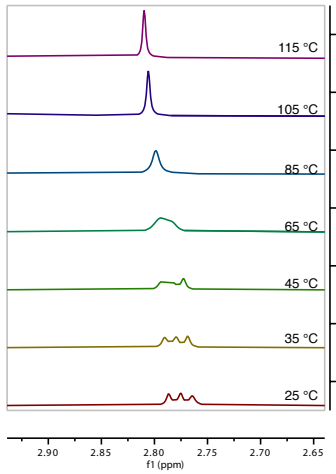
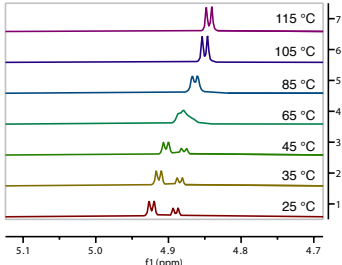
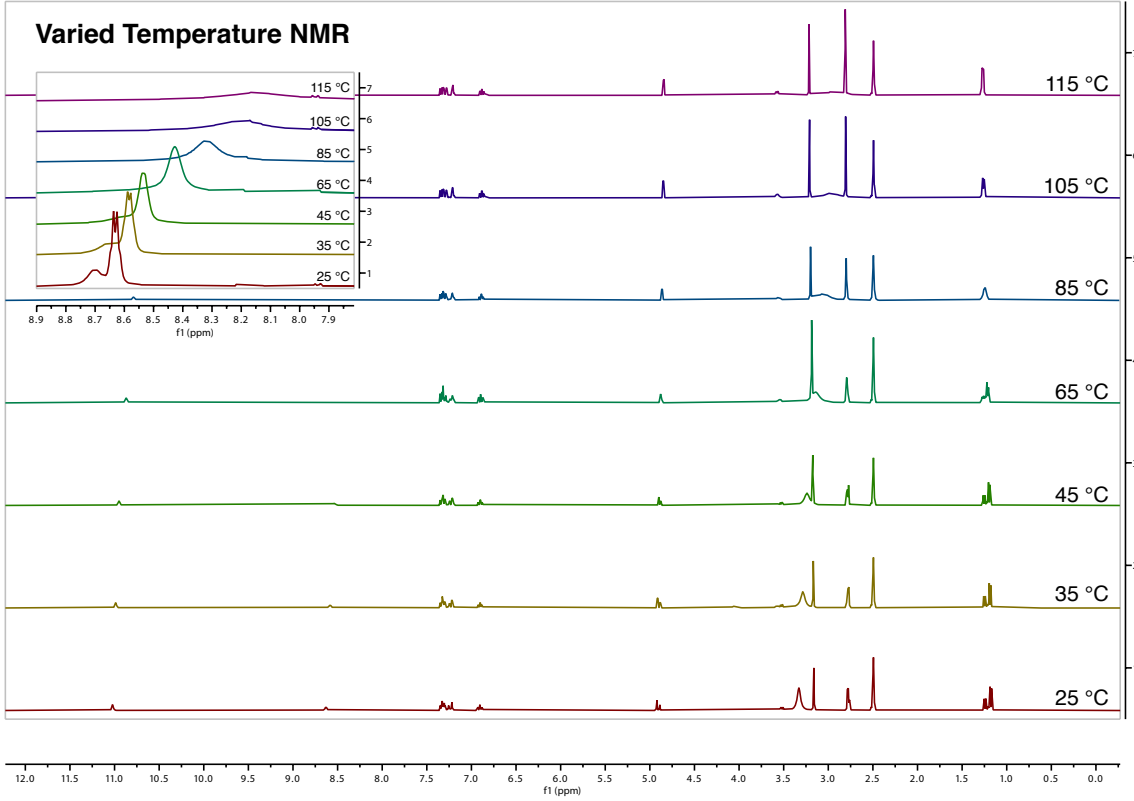


# 5F-1: 5-fluoro-indolmycin

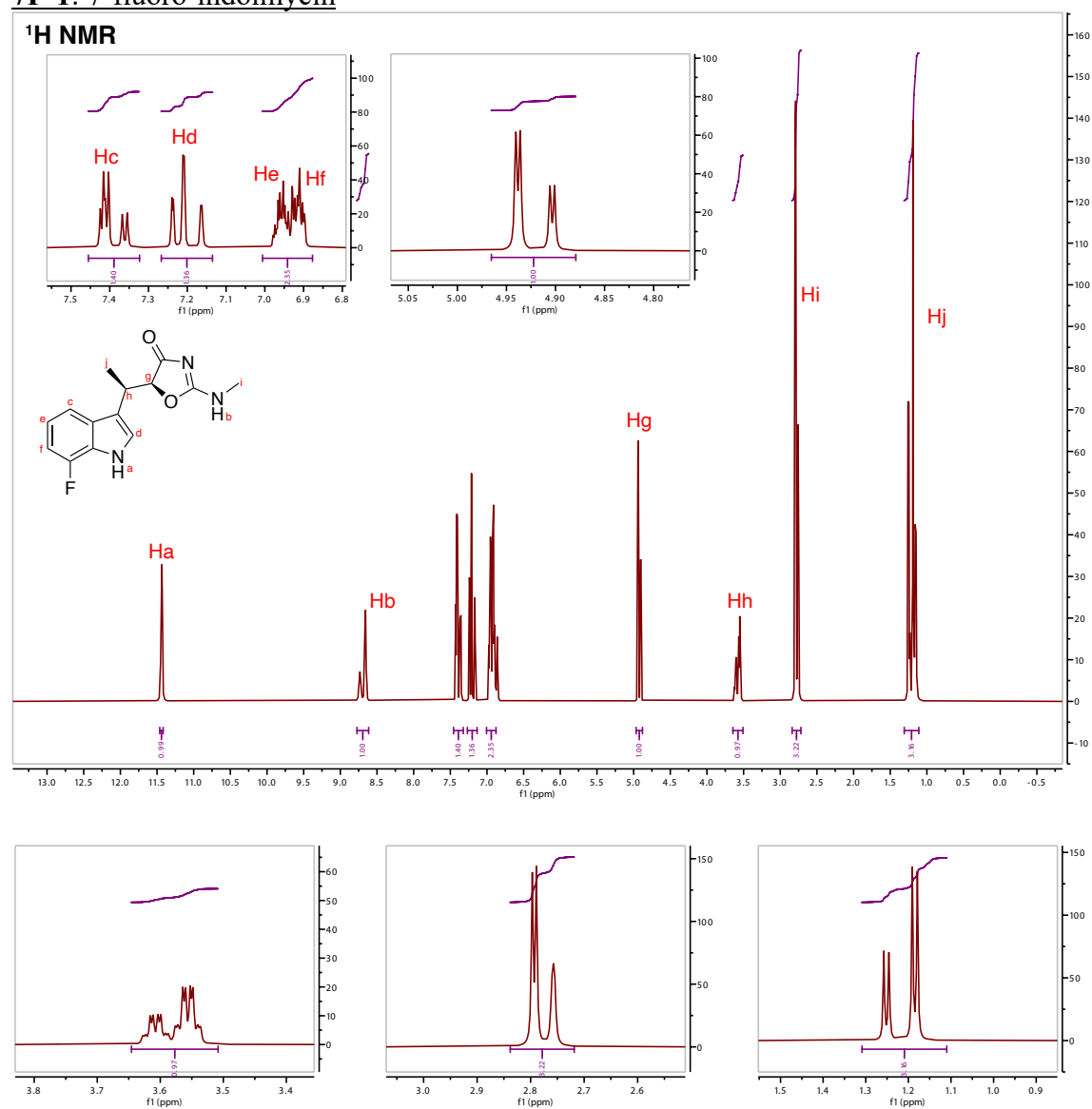


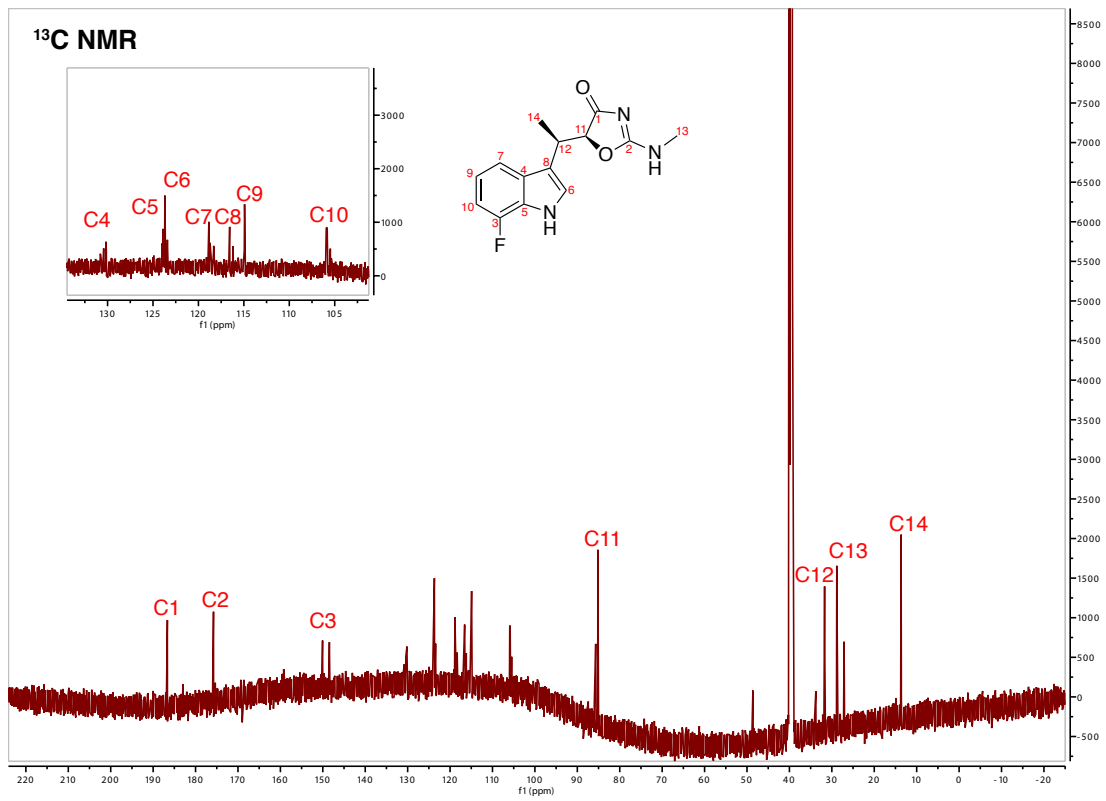




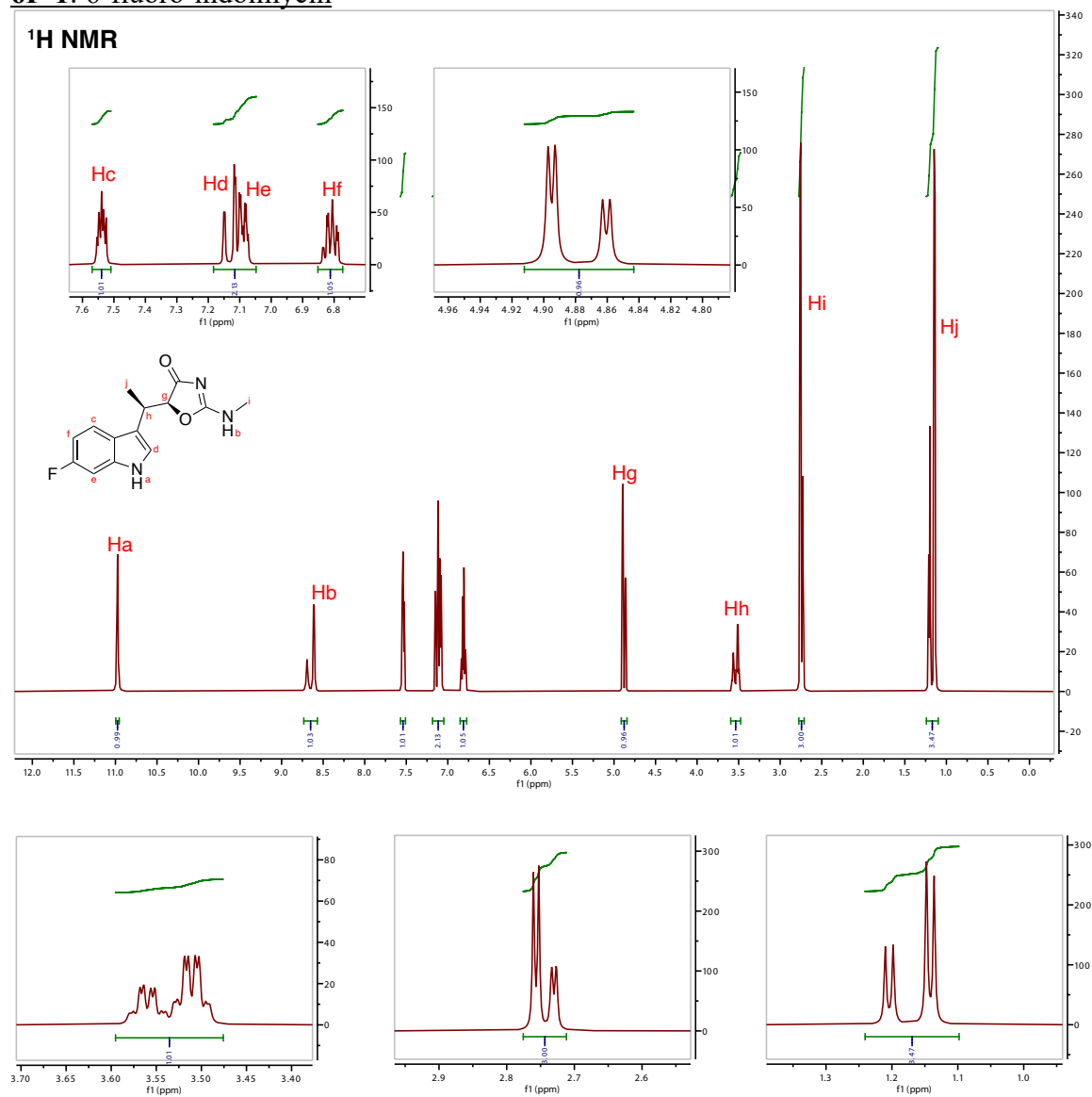


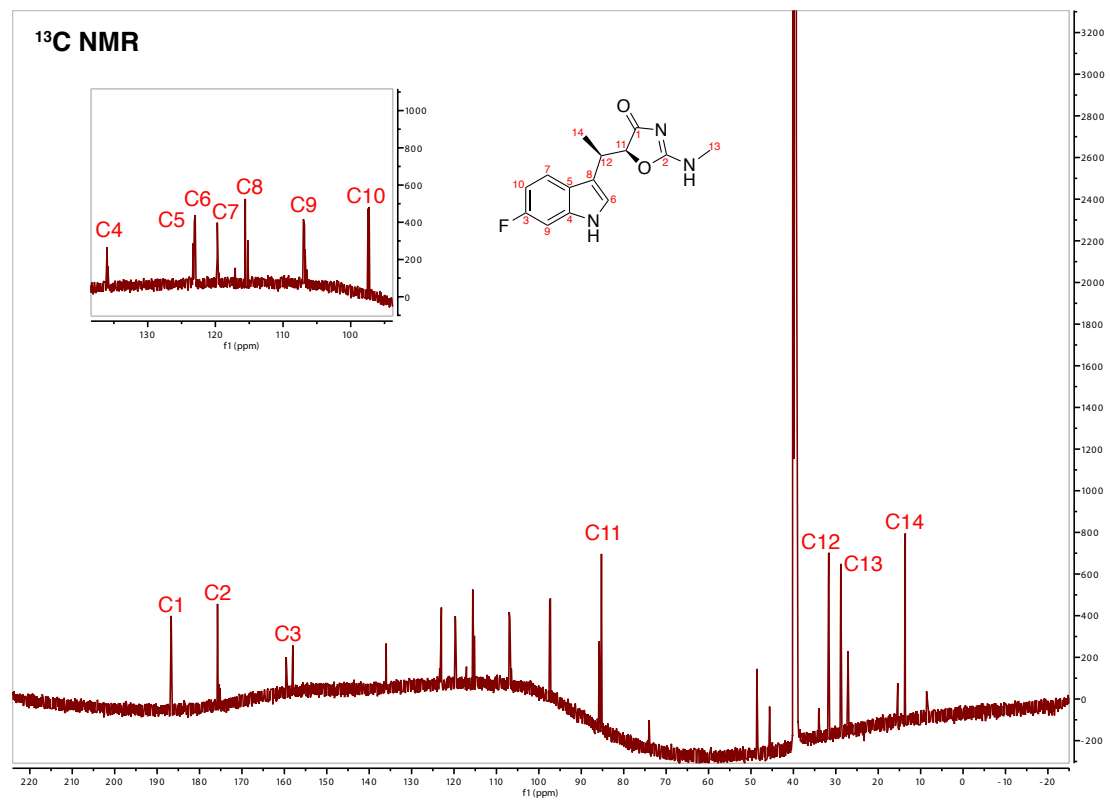
# 7F-1: 7-fluoro-indolmycin



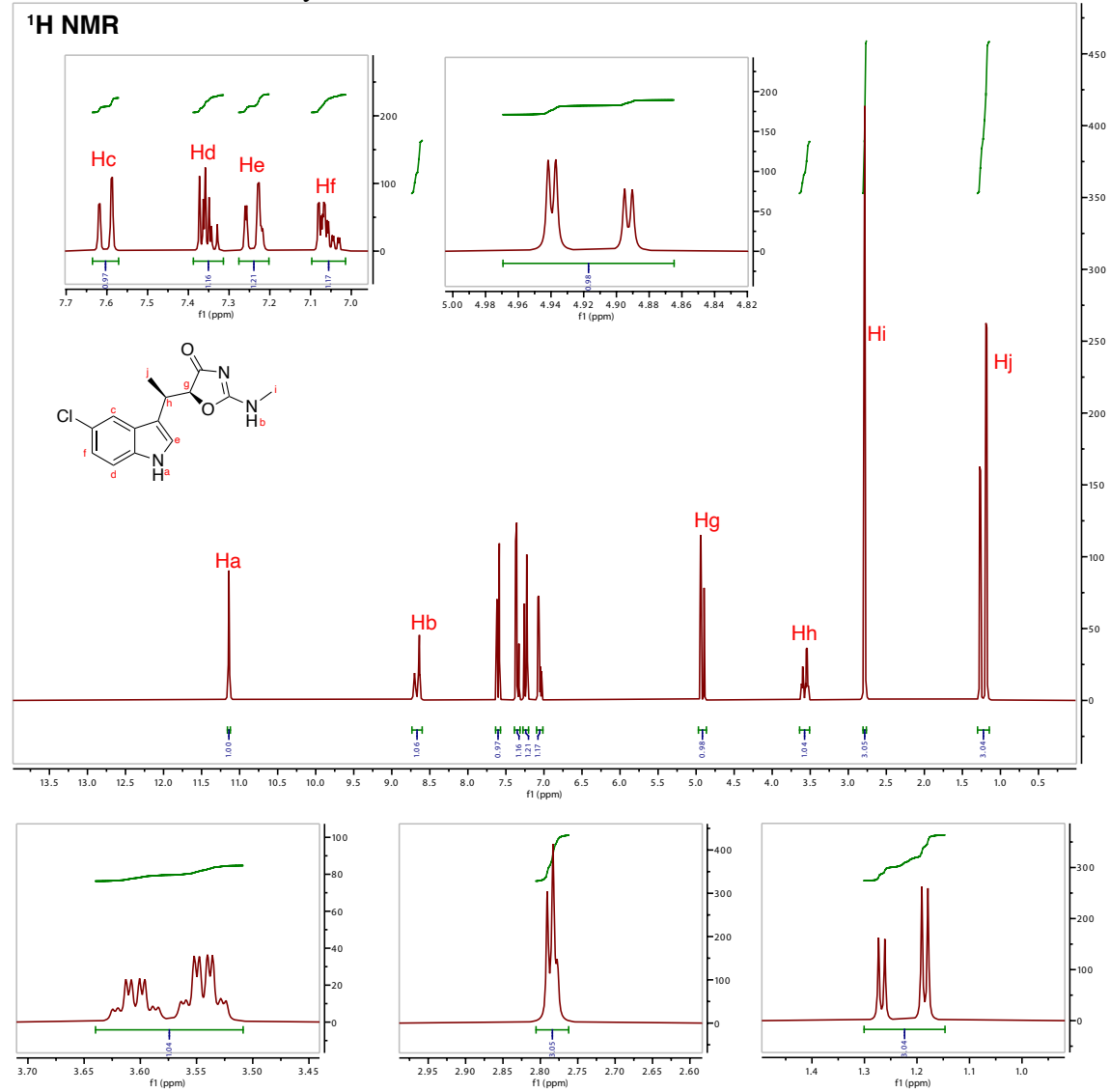


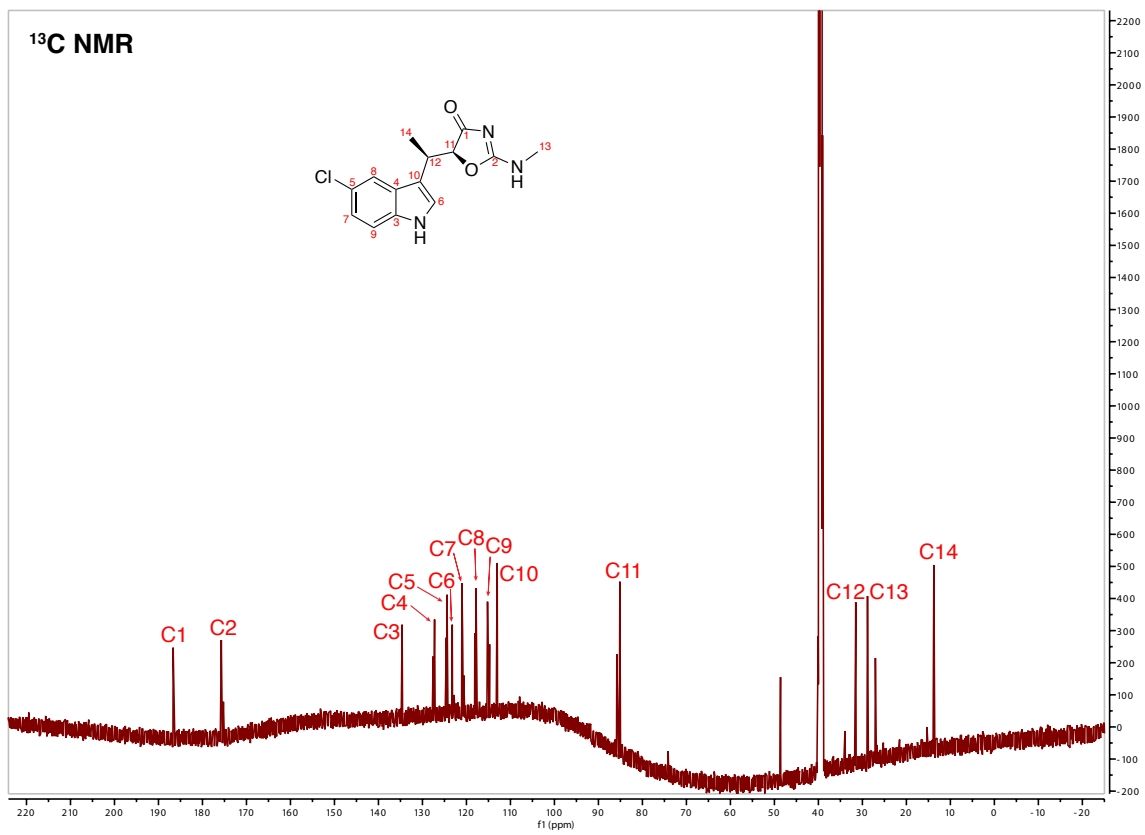
# 6F-1: 6-fluoro-indolmycin



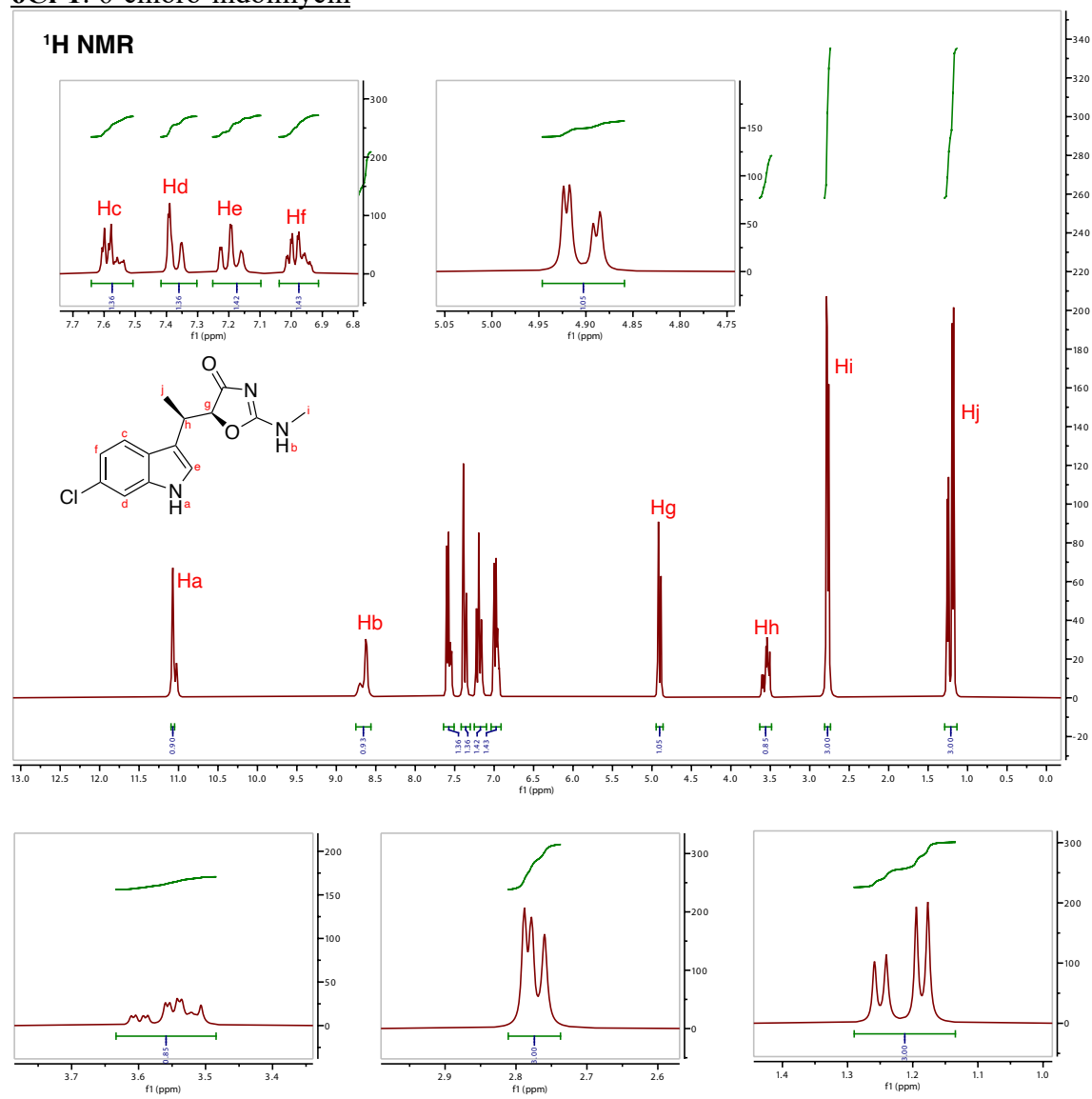


# 5Cl-1: 5-chloro-indolmycin

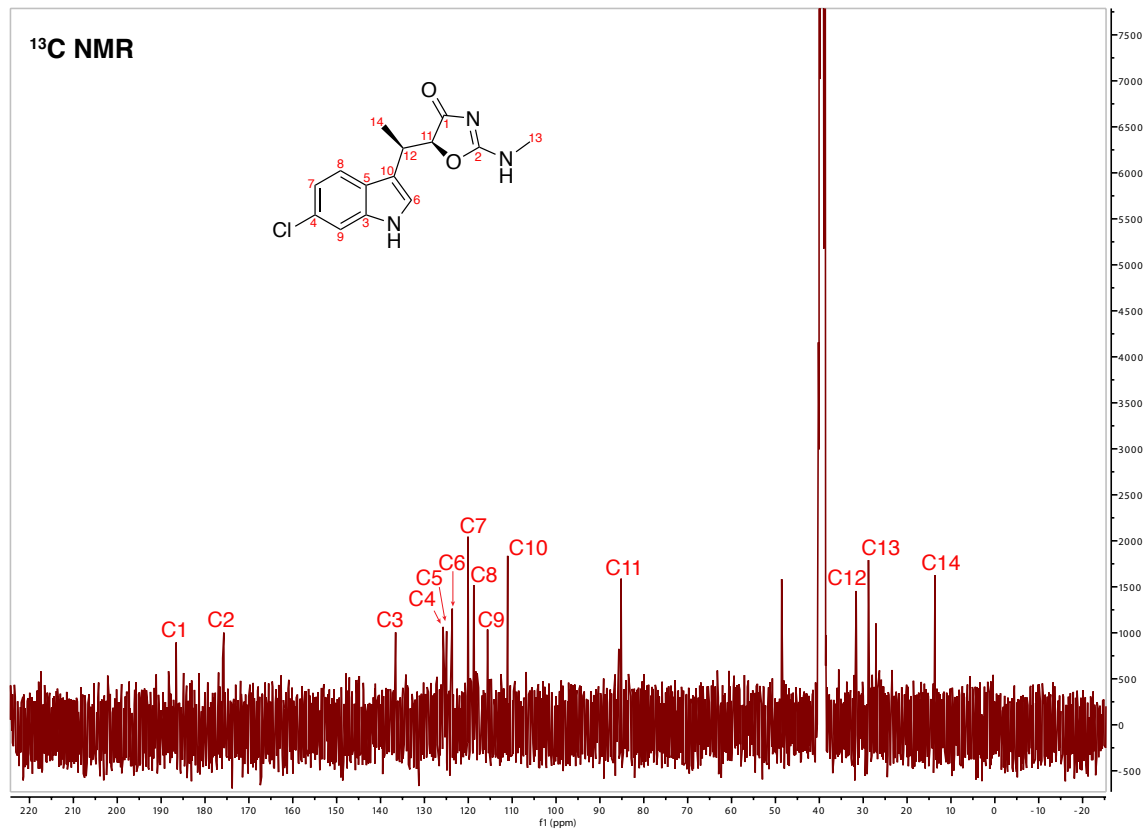
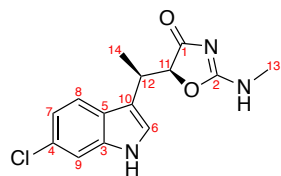




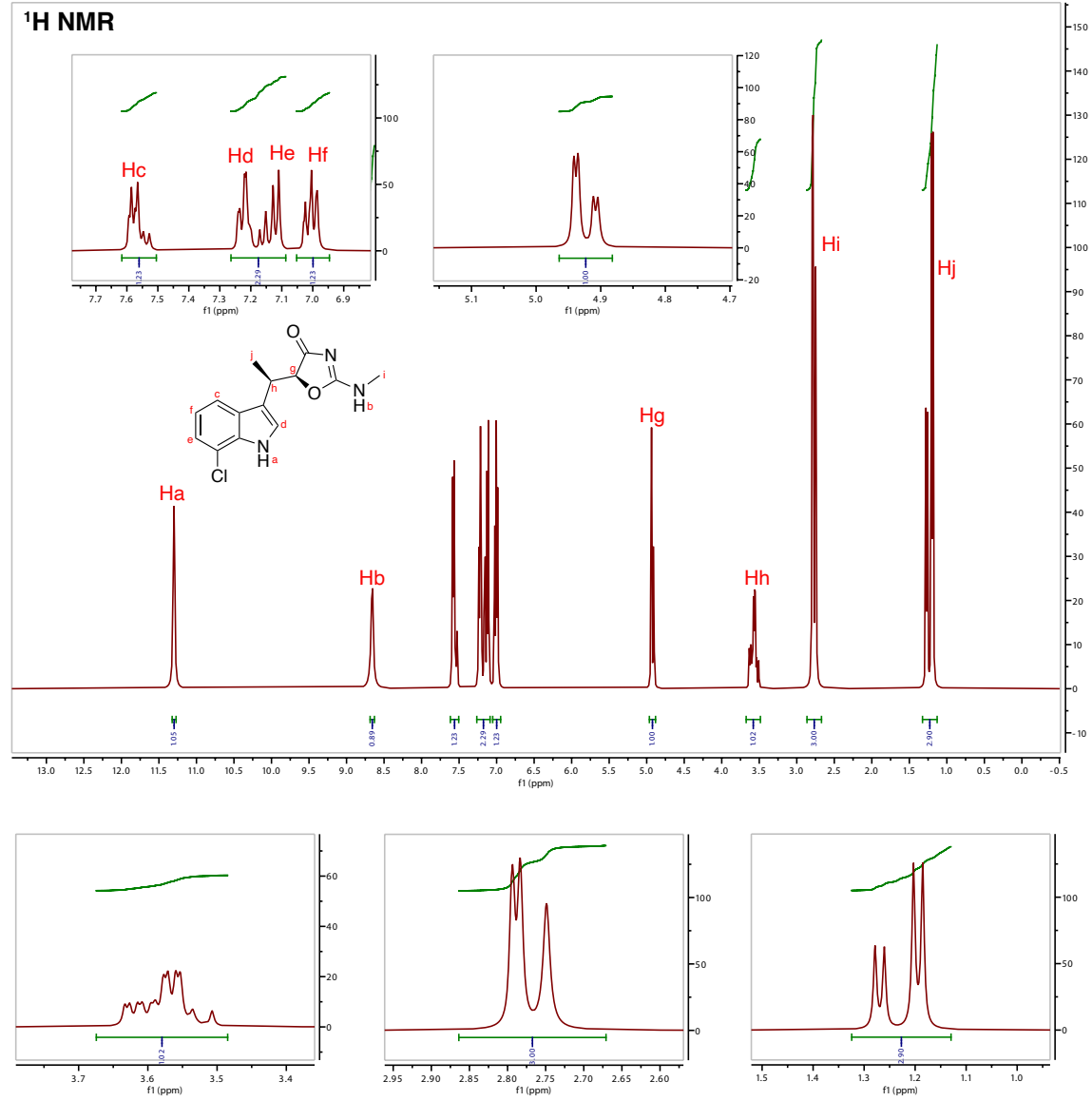
# 6Cl-1: 6-chloro-indolmycin

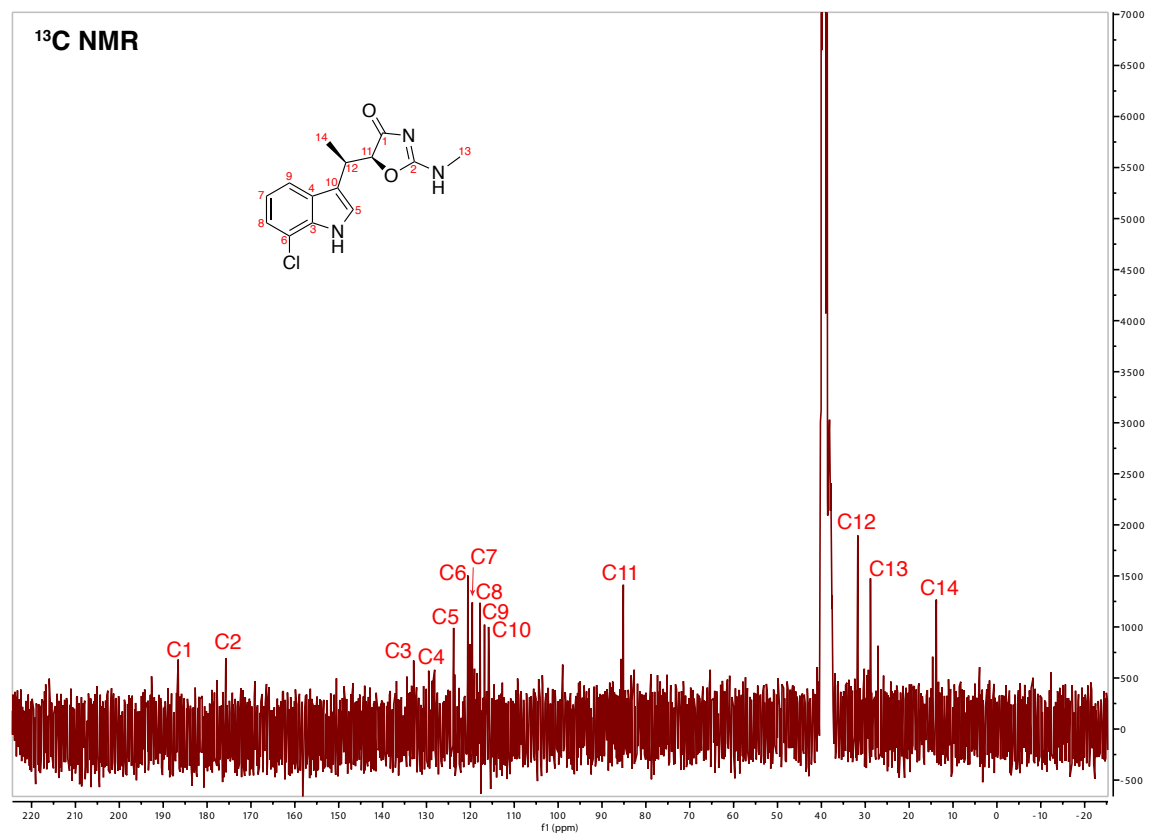


**<sup>13</sup>C NMR**



# 7Cl-1: 7-chloro-indolmycin





## References

- 1 Y.-L. Du, R. Singh, L. M. Alkhalaf, E. Kuatsjah, H.-Y. He, L. D. Eltis and K. S. Ryan, *Nat. Chem. Biol.*, 2016, **12**, 194–199.
- 2 A. Hasuoka, Y. Nakayama, M. Adachi, H. Kamiguchi and K. Kamiyama, *Chem. Pharm. Bull. (Tokyo)*, 2001, **49**, 1604–1608.
- 3 N. Sutou, K. Kato and H. Akita, *Tetrahedron Asymmetry*, 2008, **19**, 1833–1838.
- 4 M. N. Preobrazhenskaya, E. G. Balashova, K. F. Turchin, E. N. Padeiskaya, N. V Uvarova, G. N. Pershin and N. N. Suvorov, *Tetrahedron*, 1968, **24**, 6131–43.
- 5 J. Segreti, L. C. Gvazdinkas and G. M. Trenholme, *Diagn. Microbiol. Infect. Dis.*, 1989, **12**, 253–255.
- 6 Quest Graph™ IC50 Calculator, <https://www.aatbio.com/tools/ic50-calculator>, (accessed July 9, 2020).
- 7 O. Trott and A. J. Olson, *J. Comput. Chem.*, 2010, **31**, 455–461.
- 8 N. W. Moriarty, R. W. Grosse-Kunstleve and P. D. Adams, *Acta Crystallogr. D Biol. Crystallogr.*, 2009, **65**, 1074–1080.